MODELING REACTIVE TRANSPORT OF STRONTIUM-90 IN HETEROGENEOUS VARIABLY-SATURATED SUBSURFACE

By

LI WANG

A thesis submitted in partial fulfillment of
the requirements for the degree of

MASTER OF SCIENCE IN BIOLOGICAL AND AGRICULTURAL ENGINEERING

WASHINGTON STATE UNIVERSITY
Department of Biological Systems Engineering

December 2007

To the Faculty of Washington State University:

The members of the Committee appointed to examine the thesis of LI WANG find it satisfactory and recommend that it be accepted.

_____
Chair

_____

_____

_____

ACKNOWLEDGMENTS

This thesis research focuses on modeling of reactive transport of strontium-90 in heterogeneous variably-saturated subsurface at Idaho Nuclear Technology and Engineering Center (INTEC), a major facility of Idaho National Laboratory (INL), Idaho Falls, Idaho, USA. Graduate assistantship from the Inland Northwest Research Alliance (INRA) and Washington State University are greatly appreciated. During the thesis research, parallel execution of the TOUGHREACT was explored and I am grateful to the support by the National Science Foundation through TeraGrid resources provided by SDSC.

I thank Drs. Karsten Pruess, Tianfu Xu and Jerry Fairley for their valuable comments and suggestions on using TOUGHREACT, Dr. Markus Flury for the helpful discussions about questions in vadose zone hydrology, Dr. Hanxue Qiu and Mr. Limin Yang for their contributions in initiating this study, and Mr. Roger Nelson for his consistent help with managing the computing facilities and providing resources in the GIS lab where this study has been done.

I am grateful to Drs. Claudio Stöckle, Jeffrey Ullman, and Larry Hull for serving on my thesis committee and for their generous assistance. Drs. Larry Hull and Annette Schafer, both at the INL, have provided much site information and brilliant guidance on reactive-transport modeling.

Special thanks go to my major advisor Dr. Joan Wu. I appreciate her patience and her continuous and firm support. Without her, the completion of this study would have not been possible. Her hard working and persistency in conducting scientific research will always guide me in my professional career.

Last, I thank my parents for their understanding, encouragement and support, my wife Shuhui Dun, my daughter Kunxuan and my son David for being with me.

MODELING REACTIVE TRANSPORT OF STRONTIUM-90 IN HETEROGENEOUS VARIABLY-SATURATED SUBSURFACE

Abstract

by Li Wang, M.S.
Washington State University
December 2007

Chair: Joan Q. Wu

An accidental release of sodium-bearing waste (SBW) containing high concentration of Sr-90 at the Idaho Nuclear Technology and Engineering Center (INTEC), Idaho National Laboratory (INL), Idaho USA in 1972 has raised public concerns. The vadose zone at the INTEC, composed of surficial alluvium, basaltic rocks and interbedding sediments, ranges 60–270 m in thickness. In order to investigate the transport and fate of Sr-90 through this heterogeneous, variably-saturated subsurface, a *2*-dimensional model was conducted using TOUGHREACT. Four different scenarios were selected to represent different mechanisms for perched-water formation, including scenario 1 (base run), with the geometric mean of field-measured interbed permeability used for interbeds; scenario 2, the smallest field-measured interbed permeability used for interbedded sediments; scenario 3, one tenth of the smallest field-measured interbed permeability used for the top layer of interbeds at depths of 20–85 m; and scenario 4, with the smallest field-measured interbed permeability used for the top layer of basaltic rocks underlying interbeds at this range.

The results showed that different mechanisms led to different steady-state flow patterns in terms of water saturation, horizontal and vertical pore-water velocities, water residence time, and water travel time from SBW leakage to ground-water table. For all scenarios, though, water flow was vertically dominant. Scenario 2 led to larger areas of saturated zones and longest water travel time

from SBW leakage to ground-water table, while scenario 3 resulted longest water residence time for some grid blocks.

After ~15 yr, two areas of high Sr^{2+} concentration could be found at different depths beneath the SBW leakage. A small fraction of Sr plume reached ground-water aquifer in ~45 yr of simulation. After the simulated 200 yr, both Sr^{2+} concentration in solution and on exchange site still remain the highest in alluvium. Among 1.2 mol of the total Sr input, only a tiny fraction had reached ground-water aquifer, ~99.7% was on the exchange sites, ~0.3% in solution, and ~96.1% still remain in alluvium after 200 yr. The results also indicated that distribution coefficient and retardation factor for Sr^{2+} changed more than one order of magnitude for the same material because of changing concentrations of Sr^{2+} and other competing ions, both in solution and on exchange sites.

TABLE OF CONTENTS

Page

LIST OF TABLES

LIST OF FIGURES

CHAPTER ONE

INTRODUCTION

Fate and transport of radioactive nuclear contaminant through the unsaturated zone have been increasingly recognized as important processes. However, adequate modeling of these complex processes is challenging because of the naturally occurring spatial heterogeneity of subsurface geological material, and thus uncertainties in hydraulic and hydrological parameterization (Oreskes et al., 1994; MacQuarrie and Mayer, 2005). In addition, the complexity of radioactive chemical reactions and processes further adds to the challenge (Spycher et al., 2003).

Idaho Nuclear Technology and Engineering Center (INTEC, formerly the Chemical Processing Plant) is a major facility of Idaho National Laboratory (INL) situated in the Snake River Plain near Idaho Falls, Idaho, USA. Built in the early 1950s, the INTEC was initially intended for dissolving spent nuclear fuel, and has since been used to receive, store, and process legacy nuclear wastes (Cahn et al., 2006). An accidental release of approximately 70 m^3 of sodium-bearing waste (SBW) at the INTEC in 1972 has raised serious public concerns. The SBW contains 560 TBq of Sr-90 and accounts for more than 80% of the total release of Sr-90 from the INTEC. Continual transport of Sr-90 through the vadose zone poses a potential for contamination of the eastern Snake River Plain Aquifer, the major source of drinking water for the communities in the vicinity, including the city of Idaho Falls (Cahn et al., 2006).

The subsurface at the INTEC is highly complex consisting of surficial alluvium, basalt and interbedded sediments (Cecil et al., 1991; Schafer et al., 1997). As a consequence, water movement through the vadose zone is complicated with flow regimes varying substantially from one medium to another. Across the INL, water flow in alluvium is mostly vertical (Mattson et al., 2004). Within basalt, water movement is dominated by macropore flows through fractures (Nimmo et al., 2004).

Water flow patterns in interbeds were difficult to define because of the wide range of hydraulic conductivities of the media; the interbeds can serve as barriers for downward flow or paths for preferential flow (Nimmo et al., 2004). Perched zones may form along the interbed-basalt interface, while gaps in the interbeds, if combined with fractured basalt, facilitate rapid downward movement of water to the aquifer (Mattson et al., 2004).

Cecil et al. (1991) proposed four mechanisms by which perched water zones form beneath the INL: (i) low permeability of entire interbeds composed of fine sediments, (ii) low permeability of "baked" surfaces of interbeds or basalt layers by overlying lava flow, (iii) low permeability of basalt due to infilling of fractures by fine sediments, and (iv) low permeability of unfractured zone beneath rubble and fractured zones in basalt. Mattson et al. (2004) suggested that perched zones may also form above low permeability lenses inside the interbeds. In a study of inverse flow modeling, Magnuson (1995) obtained good agreement between predicted and observed perched zones by assuming low permeability of the surface of interbeds. Welhan et al. (2002) investigated the geometry of lava flows and basalt fractures at the INL, suggesting the likelihood of perched water formation along the interface between a composite zone of rubbles and fractures and the underlying unfractured zone.

Several studies have been conducted to characterize the subsurface of the INTEC and to model flow and contaminant transport. Yang (2005) used a stochastic approach to represent the heterogeneous subsurface of INTEC. Three types of materials, namely, surficial alluvium, underlying basalt, and interbedded sediments were generated using kriging. A two-dimensional model, with a lateral extent of 2000 m and extending 137 m vertically to the ground-water table, was then constructed to simulate water flow through the variably-saturated subsurface. Uncertainty analysis

suggested that water flow was most sensitive to the fraction and location of interbedded sediments (Yang, 2005).

In assessing risk of contamination, Cahn et al. (2006) simulated contaminants transport from the surficial alluvium by a hydrogeochemical model, through the vadose zone to the aquifer by a vadose-zone model, and within the aquifer by a larger-scale aquifer model. Alluvium, interbeds, and basalt were each categorized as of high or low permeability. Multiple sources of Sr-90 leakage at the INTEC were considered, and Sr-90 was found to be the only contaminant in the aquifer that would exceed drinking water standard beyond year 2095. In their study, distribution coefficients (K_d) for Sr-90 were obtained for alluvium, interbed, and basalt from experiment and literature data. Cation exchange capacity (CEC) of Sr-90 was determined by comparing available experimental data for alluvium, and was estimated from experimental data for another INL site for interbeds. However, in their contaminant transport modeling, they used CEC only for alluvium in the hydrogeochemical model, and used K_d for interbeds and basalts in the vadose-zone model and the aquifer model as in traditional transport modeling. Sensitivity analyses were performed on key hydrologic parameters, including infiltration rate, dispersivity of interbed, and geochemical parameters, such as CEC of alluvium and K_d of interbeds. Strontium transport was found most sensitive to K_d of the interbeds.

Lumping multiple reaction processes into a distribution coefficient K_d or retardation factor (R_f) in transport modeling can largely reduce data requirement and model complexity. Yet the results are likely inaccurate or even erroneous, especially for heterogeneous fields with spatially varying physical properties and large concentration gradients of contaminants, which in turn affect K_d and R_f (Hemming et al., 1997; Bunde et al., 1998; Bilgin et al., 2001; Zhu and Anderson, 2002; Zhu, 2003; Bascetin and Atun, 2006). Multi-component cation-exchange models that consider different

selectivity coefficients for different ions have proved to perform better than the traditional K_d model (Steefel et al., 2003; Hull and Schafer, 2005).

The main goal of this study was to attain a better understanding of Sr-90 transport in the variably-saturated subsurface at the INTEC as affected by spatial heterogeneity of the subsurface geological material and multi-component geochemical processes, especially cation-exchange. Four scenarios were simulated: scenario 1 (base run) with typical interbed permeability values in the literature used for the interbeds; scenario 2 with the lowest field-measured interbed permeability used for the entirety of an interbed (in accord with the aforementioned mechanism (i) for perched water formation in Cecil (1991)); scenario 3 with one tenth of the lowest measured interbed permeability used for the top layer of an interbed (mimicking mechanism (ii) of Cecil (1991)); and scenario 4 with the lowest measured interbed permeability used for the top layer of a basalt underneath an interbed (conforming with mechanism (iii) of Cecil (1991)). A coupled flow (Pruess et al., 1999) and transport model TOUGHREACT (Xu and Pruess, 2001; Xu et al., 2004) was used to simulate the fate and transport of Sr-90 under different representations of the proposed mechanisms for formation of perched water zones at the INTEC.

CHAPTER TWO

METHODOLOGY

2.1 Study Area

The INTEC site (Fig. 1) is located within the semiarid sagebrush desert on the upper Snake River Plain at an average altitude of 1500 m a.s.l. The vadose zone, consisting primarily of surficial alluvium, fractured basalt and interbedded sediment, ranges 60–270 m in thickness. The hydraulic properties of the basalt are highly anisotropic. Layered basalt can have high horizontal permeability, and basalt with fractures containing sediment infilling and fracture wall coatings often show a significant decrease in vertical permeability (Hull et al., 1999). Average basalt permeability is on the order of 10^{-9} m^2, while the average permeability in sediment interbeds is on the order of 10^{-14} m^2 (Schafer et al., 1997). The sedimentary units, though generally thinner and less widespread than in many other sites of the INL, are frequently associated with relatively high water saturation, known as perched water zones.

Recharge that influences contaminant transport at the INTEC comes from both natural sources (precipitation and the discharge from the adjacent Big Lost River) and anthropogenic sources (water supply leaks, irrigation, sewage treatment and percolation ponds) (Hull et al., 1999). Long-term annual precipitation averages 0.22 m, and net recharge is about 0.18 m yr^{-1} (Cahn et al., 2006).

A *2*-dimensional model domain (A–A′ transect, Fig. 1), with a lateral extent of 1000 m extending vertically to the ground-water table (−137.6 m) modified from Yang (2005), was chosen (Fig. 2). The distribution of basalt and sediment interbedding was determined using indicator kriging with a probability cutoff value of 0.5 (Yang, 2005). The total number of grid blocks was 65×242, with constant horizontal grid spacing of 15.24 m, and varying vertical grid spacing from 0.3 to 3.0 m. Four observation points were selected below the SBW leakage location: Obs. 1 in alluvium, Obs.

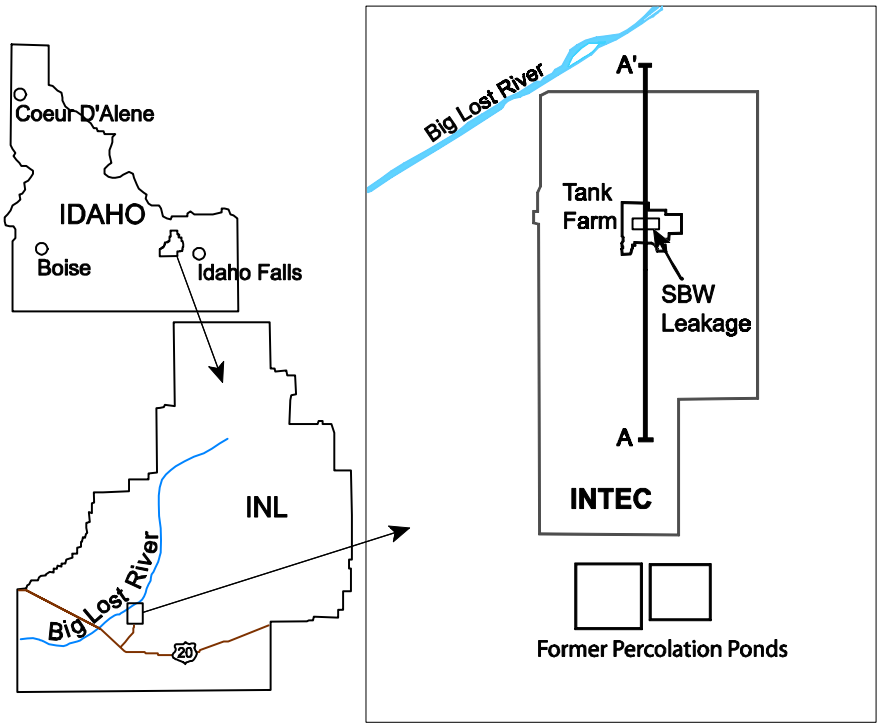

Figure 1. Study site. A–A′ shows the cross section modeled in this study.

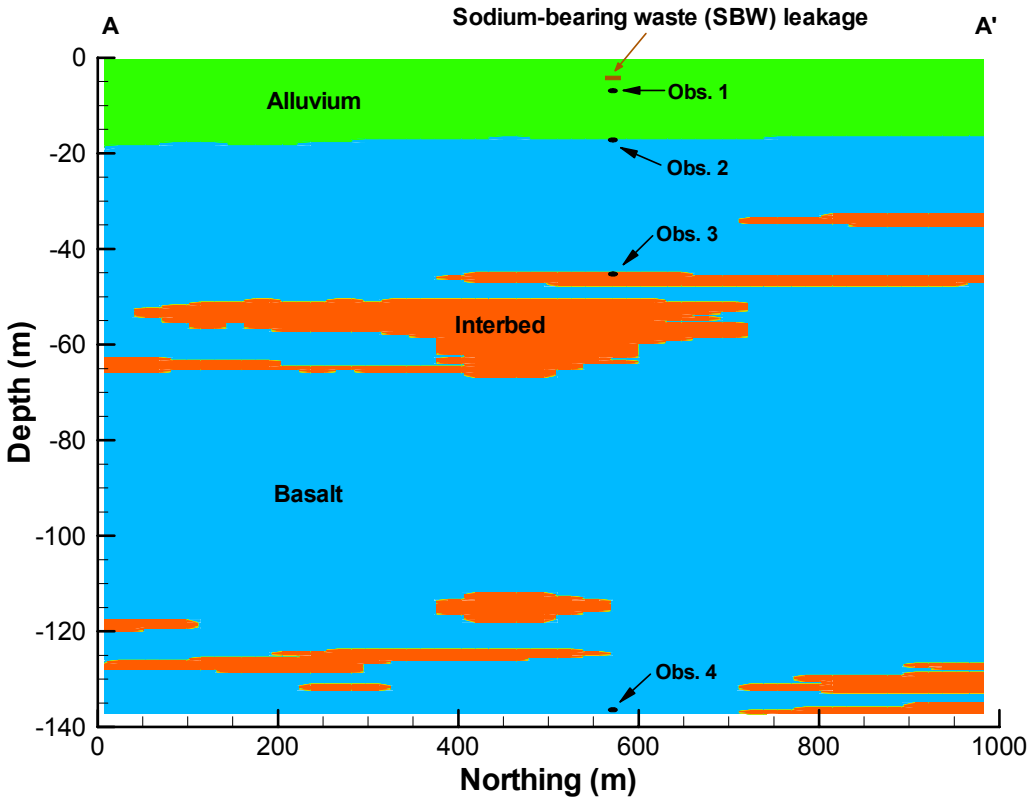

Figure 2. Model domain with geostatistically interpreted geological stratigraphy by Yang (2005).

2 in uppermost basalt, Obs. 3 in uppermost interbed, and Obs. 4 at 1 m above ground-water level (Fig. 2).

The assumptions and simplifications made in this study included: (i) gas was in ideal state with total gas pressure equal to the sum of partial pressures of air and vapor; (ii) chemical reactions and processes were at local equilibrium and took place under isothermal conditions at 25°C; and (iii) hysteresis of unsaturated flow, permeability change due to chemical reactions, and radioactive decay were not considered during the simulation.

2.2 Governing Equations

The mass conservative equations describing the flow system are given by (Pruess et al., 1999)

$$\frac{\partial M^{\kappa}}{\partial t} = -\nabla \cdot F^{\kappa} + q^{\kappa} \qquad [1]$$

$$M^{\kappa} = \phi \sum_{\beta} S_{\beta} \rho_{\beta} X_{\beta}^{\kappa} \qquad [1a]$$

$$F^{\kappa} = \sum_{\beta} u_{\beta} \rho_{\beta} X_{\beta}^{\kappa} \qquad [1b]$$

$$u_{\beta} = -k \frac{k_{r\beta}}{\mu_{\beta}} \left(\nabla P_{\beta} - \rho_{\beta} g \right) \qquad [1c]$$

where M^{κ} is mass accumulation (Mg m^{-3}), F^{κ} is fluid mass flux (Mg m^{-2} s^{-1}), u_{β} is the Darcy velocity (m s^{-1}), q is a source or sink term (Mg m^{-3} s^{-1}), ϕ is the porosity of the medium, S is degree of saturation, ρ is density (Mg m^{-3}), X is mass fraction, k is absolute permeability (m^2), k_r is relative permeability, P is pressure (Pa), and μ is viscosity (Mg m^{-1} s^{-1}). The superscript κ indicates a flow component (water or air), and subscript β represents a fluid phase (liquid or gas).

The chemical transport equation in liquid phase of unit volume is written as (Xu et al., 1999; Xu et al., 2004)

$$\frac{\partial}{\partial t}(\phi S_l C_j) = \nabla\cdot(\phi S_l \tau D \nabla C_j) - \boldsymbol{u}\cdot\nabla C_j + w(C_j^* - C_j) + \phi S_l R_j \qquad j = 1, 2, ..., N_c \qquad [2]$$

where N_c is the number of chemical components, C_j is the total dissolved concentration (mol L^{-1}) of component j, C_j* is the dissolved concentration (mol L^{-1}) of component j in fluid source with volume flux w (s^{-1}), τ is medium tortuosity, D is diffusion coefficient (m^2 s^{-1}), and R_j is the reactive sink or source term (mol L^{-1} s^{-1}).

A local equilibrium cation-exchange model was considered in this study. A cation-exchange reaction is described as (Xu et al., 2004)

$$\frac{1}{i}\mathrm{A}^{i+} + \frac{1}{j}\mathrm{BX}_j \rightleftharpoons \frac{1}{i}\mathrm{AX}_i + \frac{1}{j}\mathrm{B}^{j+} \qquad [3]$$

where A and B are cations with charges i and j, respectively, and A is the reference cation (Na^+ in this study). X denotes a negatively charged exchange site on the surface of clay particles.

The cation exchange equilibrium constant, also referred to as selectivity (or exchange) coefficient, is calculated as (Xu et al., 2004)

$$K^*_{\mathrm{A\backslash B}} = \frac{f_\mathrm{A}^{1/i}\cdot a_\mathrm{B}^{1/j}}{f_\mathrm{B}^{1/j}\cdot a_\mathrm{A}^{1/i}} = \frac{f_\mathrm{A}^{1/i}\cdot(C_\mathrm{B}\gamma_\mathrm{B})^{1/j}}{f_\mathrm{B}^{1/j}\cdot(C_\mathrm{A}\gamma_\mathrm{A})^{1/i}} \qquad [4]$$

where f_A and f_B represent the activities of exchanged cations A and B, and are assumed to equal the equivalent fractions of exchanged cations A and B, respectively, a_A and a_B are the activities of dissolved species A and B, respectively, which are the products of concentrations (C, in mol L^{-1}) and

activity coefficients (γ) of A and B, and are unitless. The activity coefficient is calculated by the extended Debye-Huckel equation (Xu et al., 2004).

Given selectivity coefficients and dissolved concentrations of the cations, the equivalent fraction f can be solved for each cation with $\sum_{k=1}^{N_w} f_k = 1$, where N_w is the total number of exchanged cations.

The concentration w_k (mol L^{-1} of fluid) of the k-th exchanged cation is calculated as (Xu et al., 2004, p. 157)

$$w_k = f_k \rho_s \frac{CEC(1-\phi)}{100 z_k \phi S_l} \qquad k = 1, 2, ..., N_w \qquad [5]$$

where CEC is the cation exchange capacity of the medium ($cmol_c$ kg^{-1}). The term S_l in Eq. [5] is added for variably-saturated condition (L. Hull and A. Schafer, INL, personal communication, 2006).

Distribution coefficient is calculated by

$$K_d = \frac{S}{C} = \frac{w \phi S_l}{C \rho_s (1-\phi)} \qquad [6]$$

where K_d is the equilibrium distribution coefficient (L kg^{-1}), S is the mass of adsorbed ion per unit mass of solid phase (mol kg^{-1} solid), C is the concentration of ion in solution (mol L^{-1}), and w is the concentration of exchanged cation (mol L^{-1} liquid).

Retardation factor is determined from

$$R_f = 1 + \frac{1-\phi}{\phi S_l} \rho_s K_d = 1 + \frac{w}{C} \qquad [7]$$

2.3 Model Settings

2.3.1 General Settings and Simulation Scenarios

The sequential non-iterative approach was used for the reactive transport modeling, with a total simulation time of 200 yr. To retain accuracy of transport simulation, the Courant number was set to 0.3 following Xu et al. (1999). The Courant number is defined as

$$C_r = \frac{v\Delta t}{\Delta L} \quad [8]$$

where v is the fluid pore velocity (m s^{-1}), Δt is the maximum time step (s), and ΔL is the grid spacing (m) in x or z direction.

Four scenarios of low-permeability zones were simulated. They are: scenario 1 (base run), with a geometric mean of field-measured interbed permeability used for the entirety of an sediment interbed; scenario 2, with the lowest field-measured interbed permeability used for the entirety of an interbed; scenario 3, with one tenth of the lowest measured interbed permeability used for the top layer of an interbed between bottom of alluvium (~20 m) and 85 m below ground surface; and scenario 4, with the lowest field-measured interbed permeability used for the top layer of a basalt underneath an interbed in the range of 20–85 m below ground surface (Table 1).

Kriging results of Yang (2005) suggest that only the interbeds at 40–60 m below ground surface were relatively continuous. Yet others (e.g., Schafer et al., 1997; Cahn et al., 2006) reported that perched water had formed in a broader range of 20–85 m below land surface, possibly as a consequence of the lateral extension of the interbeds.

The relative permeability function was described by the van Genuchten-Mualem model (van Genuchten, 1980; Pruess et al., 1999; Schaap and van Genuchten, 2006) and the capillary pressure

Table 1. Major properties of the geologic materials at the Idaho Nuclear Technology and Engineering Center (INTEC), following Cahn et al. (2006).

Medium simulated[†]	Porosity	Particle density	Permeability	S_{lr}[‡]	van Genuchten parameters		CEC[§]
					α	*m*	
		$Mg\ m^{-3}$	m^2		m^{-1}		$cmol_c\ kg^{-1}$
Alluvium, in all four scenarios	0.32	2.65	9.17×10^{-12}	0.020	11.27	0.338	5.0
Interbed, in 1, 3, and 4	0.47	2.65	2.18×10^{-13}	0.020	0.757	0.227	21.0
Interbed_l, in 2	0.49	2.65	3.00×10^{-15}	0.0002	0.01	0.275	21.0
Interbed_tl, in 3	0.05	2.65	3.00×10^{-16}	0.142	1.066	0.343	21.0
Basalt, in all four scenarios	0.05	2.65	H[¶]: 3.00×10^{-14} V[#]: 3.00×10^{-13}	0.001	10.0	0.600	0.01
Basalt_tl, in 4	0.03	2.65	3.00×10^{-15}	0.050	5.0	0.500	0.01

[†] The four scenarios are: 1. base run with a geometric mean of interbed permeability used for the entirety of all sediment interbeds, 2. with lowest measured interbed permeability used for the entirety of interbed, 3. with one tenth of the lowest measured interbed permeability used for the top layer of any interbed at the depths of 20–85 m, and 4. with lowest measured interbed permeability used for the top layer of any basalt underneath an interbed in this depth range.

[‡] Residual water saturation.

[§] Cation exchange capacity.

[¶] Horizontal.

[#] Vertical.

function by van Genuchten function (van Genuchten, 1980; Pruess et al., 1999). Diffusion coefficient of the medium for aqueous species was assumed to be 2.0×10^{-9} m^2 s^{-1}.

2.3.2 Boundary Conditions

The side boundaries of the model domain were set as no-flow boundaries, since the water flow in this region is dominated by vertical movement (Magnuson, 1995, p. 16; Yang, 2005, p. 14; Cahn et al., 2006, p. 8-5). The ground-water level was used as a constant-head boundary for the bottom. The top boundary was a constant-flux boundary with a flux of 0.18 m yr^{-1}, the long-term average annual recharge.

The composition of the recharge water at the top boundary (Table 2) was extracted from Cahn et al. (2006). Nitrate was considered as a conservative species and can be used to corroborate the adequacy of simulated water flow and cation transport. The partial pressure of CO_2 (g) was around 0.01 bar (Cahn et al., 2006).

2.3.3 Initial Conditions

The initial flow system on 1 Jan. 1971 (time 0), one year prior to the SBW release, was assumed to be at steady state with a constant infiltration rate of 0.18 m yr^{-1}. The condition was reached by first simulating a variably-saturated flow system from a gravity-capillary-equilibrium state, and then a flow system of water and air, until steady state was reached. Appendix A includes a utility code in Fortran for combining the outputs from the variably-saturated system, such as permeability and saturation, with general inputs (pressure, temperature) for the flow system (Appendix A1). Water chemistry of the initial pore water was assumed to be the same as the recharge water (Table 2). Minerals were assumed to be at equilibrium state, including 5% (in volume) of calcite and no gibbsite. The initial partial pressure of CO_2 (g) was set as 0.01 bar.

Table 2. Chemical composition of recharge water, initial water and sodium-bearing waste (SBW) solution following Cahn et al. (2006).

	Concentration	
Components	Recharge and initial water	SBW solution
	mol L^{-1}	
H^+	5.369×10^{-8} (pH = 7.27)	1.50
Ca^{2+}	1.64×10^{-3}	1.0×10^{-17}
Na^+	3.3×10^{-4}	1.50
Al^{3+}	2.0×10^{-8}	0.50
Cs^+	5.0×10^{-16}	2.019×10^{-5}
Sr-90	5.0×10^{-16}	1.74×10^{-5}
HCO_3^-	3.64×10^{-3}	1.0×10^{-17}
NO_3^-	1.0×10^{-9}	4.50
Cl^-	3.30×10^{-4}	1.0×10^{-17}
Br^-	1.0×10^{-12}	3.3×10^{-4}

2.3.4 Source Term

The leakage of SBW during 1972 was simulated as a 50-d constant-rate release at a depth of 4.2 m over an area of 609.6 m^2, starting 0000 h on 1 Jan. 1972. The SBW contained high concentrations of Na and Sr-90, and was highly acidic (Table 2).

2.3.5 Cation Exchange

The effect of stable Sr on Sr-90 transport has been found insignificant (Cahn et al., 2006) and was therefore neglected in this study. The reference cation was Na^+, and the cation exchange reactions considered were:

$$Na^+ + HX \rightleftharpoons NaX + H^+ \quad [9a]$$

$$Na^+ + \frac{1}{2}CaX_2 \rightleftharpoons NaX + \frac{1}{2}Ca^{2+} \quad [9b]$$

$$Na^+ + CsX \rightleftharpoons NaX + Cs^+ \quad [9c]$$

$$Na^+ + \frac{1}{2}SrX_2 \rightleftharpoons NaX + \frac{1}{2}Sr^{2+} \quad [9d]$$

$$Na^+ + \frac{1}{3}AlX_3 \rightleftharpoons NaX + \frac{1}{3}Al^{3+} \quad [9e]$$

The selectivity coefficients ($K_{Na\backslash B}$) defined by Eq. [4] were from Appelo and Postma (1996) (Table 3).

2.3.6 Model Outputs

Model outputs for water flow included degree of saturation for each grid block and pore water velocity from grid block to grid block. Average pore water velocities ($\bar{v}_x$, and $\bar{v}_z$ for x and z directions, respectively, m s^{-1}) of each grid block were calculated by averaging pore water velocities across the boundaries of the grid block, using a shareware EXT for TOUGH2 data post-processing

Table 3. Cation exchange selectivity coefficients. The selectivity value for H^+ is from Cahn et al. (2006), and values for other cations are based on Appelo and Postma (1996).

Cation B	$K_{Na\backslash B}$
Na^+	1.0
Cs^+	0.08
Ca^{2+}	0.4
Al^{3+}	0.6
Sr-90	0.35
H^+	7.7×10^5

(http://www-esd.lbl.gov/TOUGH2/PROGRAMS/FREEPROGRAMS.html, 09/20/2007). Water residence time (t, d) was also calculated to compare the effect of the alternative mechanisms of perched-water formation on water flow. Water residence time of a grid block was estimated as

$$t = \frac{V}{86400(|\bar{Q}_x| + |\bar{Q}_z|)} = \frac{\Delta x \cdot \Delta z}{86400(\Delta x \cdot |\bar{v}_z| + \Delta z \cdot |\bar{v}_x|)} \quad [10]$$

where $V = \Delta x \cdot \Delta y \cdot \Delta z \cdot \phi \cdot S_l$ is the volume of water in a grid block (m^3), $\bar{Q}_x = \Delta y \cdot \Delta z \cdot \bar{v}_x \cdot \phi \cdot S_l$ and $\bar{Q}_z = \Delta x \cdot \Delta y \cdot \bar{v}_z \cdot \phi \cdot S_l$ are average water flow rates through the grid block ($m^3\ s^{-1}$) in x and z directions, respectively, Δx, Δy and Δz are the grid block sizes (m). The modification of EXT codes is presented in Appendix A2 for calculating t.

Model outputs for reactive transport of Sr-90 included mass balance of Sr for selected times, the concentrations of its aqueous species (Sr^{2+}, $SrCO_3(aq)$, $SrNO_3^+$, and $SrOH^+$) and exchanged species (SrX_2) with time for the four specified observation points, and for every grid block for selected times (2.5, 5, 15, 30, 50, 60, 200 yr). The effect of different mechanisms of perched-water formation on Sr transport was evaluated. In addition, Sr^{2+} and NO_3^- transport was compared, and time-varying K_d and R_f for Sr^{2+} were estimated to assess the retardation effect of cation exchange. Codes for calculating K_d and R_f for every grid block at selected times is presented in Appendix A3 and modification of TOUGHREACT codes on mass balance calculation is listed in Appendix B. Sample pages of model inputs and outputs are listed in Appendix C and D, respectively.

CHAPTER THREE

RESULTS AND DISCUSSION

3.1 Steady-state Water Flow

3.1.1 Steady-state Water Saturation

Four scenarios were simulate to test different hypothetical mechanisms of perched-water formation, including base run with geometric mean of measured permeability used for the interbeds, scenario 2 with the smallest measured permeability used for the interbeds, scenario 3 with one tenth of the smallest permeability used for the top layer of interbeds, and scenario 4 with the smallest measured permeability used for the top layer of basalts beneath interbed. There was substantial difference in the resultant steady-state water saturation under different scenarios (Fig. 3). The minimum degree of water saturation of a grid block within the domain was 0.13 for the base run, 0.22 for scenario 2, 0.11 for scenario 3, and 0.12 for scenario 4 (Table 4).

The location of saturated zones of the interbeds differ in different simulation scenarios. The interbeds are mainly saturated near their interfaces with the underlying basalts in the base run; they were, however, nearly completely saturated in scenario 2. Saturated zones formed at the interfaces with both underlying and overlying basalts in scenario 3. In scenario 4, the position of saturated zones was similar to that in the base run, but the saturated areas were slightly larger (Fig. 3). The degree of water saturation for basalts ranged 0.20–0.25 across most of the model domain. The vertical stripes (higher saturation, 0.25–0.30, in most cases; or lower saturation, 0.15–0.2, in two cases in scenarios 3 and 4) occurred where the interbed-basalt interface was not smooth. Water saturation of the alluvium was nearly the same in all scenarios, because of its uniform hydraulic properties, relatively simple configuration and position near the top boundary within the model domain.

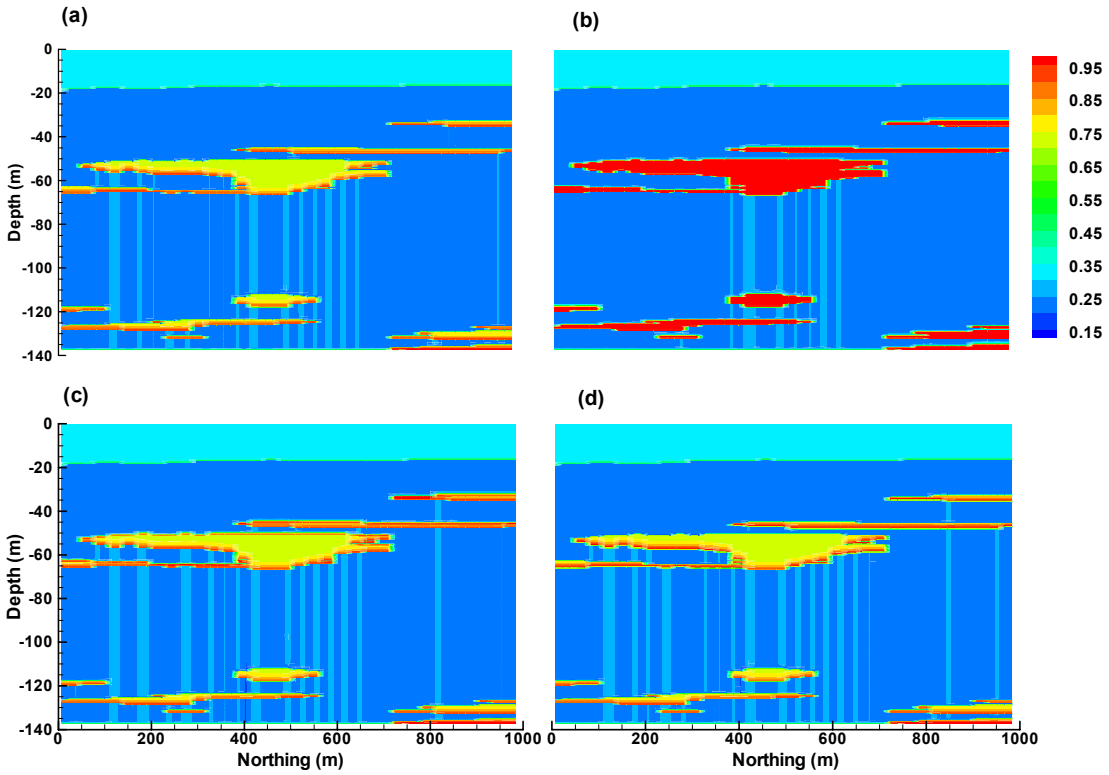

Figure 3. Steady-state water saturation for (a) base run, (b) scenario 2, (c) scenario 3, and (d) scenario 4.

Table 4. Steady-state water saturation.

	Water saturation				
Scenario	Mean	Median	SD	Minimum	Maximum
1 (base run)	0.34	0.25	0.20	0.13	0.99
2	0.38	0.25	0.26	0.22	1.00
3	0.35	0.25	0.21	0.11	1.00
4	0.35	0.25	0.21	0.12	0.99

The SBW leakage caused minor changes to the field of water saturation with a small peak of water saturation migrating downward with time and a steady state recovered after ~6 yr of simulation time. The effect of the SBW leakage on water flow and contaminant transport during the 200-yr simulation appeared minor.

3.1.2 Horizontal Velocity of Water Flow

Scenarios 1, 2, and 4 resulted in small values of horizontal velocity of water flow comparing with scenario 3. In all four scenarios, the relatively higher horizontal velocity of water flow occurred around the horizontal interfaces of alluvium-basalt, or interbed-basalt. This was because the higher contrasts of saturation and capillary pressure between different materials caused higher hydraulic gradients at these interfaces. For the base run and scenarios 2 and 4, the horizontal pore water velocity ($\bar{v}_x$) ranged from -9.8×10^{-9} (negative sign suggesting flow to the left) to $+4.7\times10^{-8}$ (positive sign suggesting flow to the right); for scenario 3, $\bar{v}_x$ ranged -4.5×10^{-7} –4.7×10^{-7} m s^{-1}, one order of magnitude larger than in other three scenarios (Fig. 4, Table 5).

3.1.3 Vertical Velocity of Water Flow

Vertical water flow was exclusively downward (represented by negative values) as a result of the constant-flux top boundary (Fig. 5). For the base run, the vertical velocity ($\bar{v}_z$) ranged from -8.2×10^{-7} to -7.0×10^{-9} m s^{-1}; for scenario 2, $\bar{v}_z$ ranged from -5.7×10^{-7} to -8.0×10^{-9} m s^{-1}; for scenario 3, $\bar{v}_z$ ranged from -8.9×10^{-7} to -4.8×10^{-9} m s^{-1}; and for scenario 4, $\bar{v}_z$ ranged from -8.9×10^{-7} to -5.4×10^{-9} m s^{-1} (Table 6). The magnitude of $\bar{v}_z$ was mostly larger than that of $\bar{v}_x$ except for certain grid blocks in scenario 3.

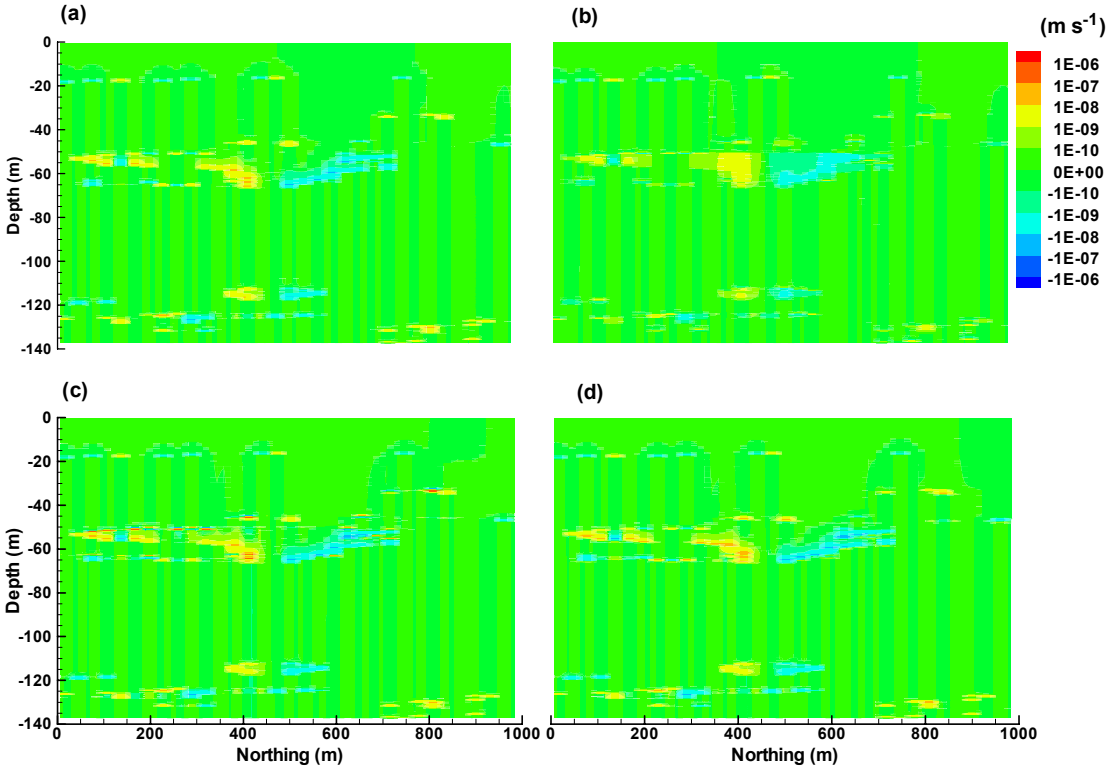

Figure 4. Steady-state horizontal pore water velocity for (a) base run, (b) scenario 2, (c) scenario 3, and (d) scenario 4.

Table 5. Steady-state horizontal pore-water velocity.

Scenario	Horizontal pore-water velocity				
	Mean	Median	SD	Minimum	Maximum
	$m\ s^{-1}$				
1 (base run)	-6.0×10^{-12}	2.2×10^{-17}	1.4×10^{-9}	-3.2×10^{-8}	2.9×10^{-8}
2	-7.0×10^{-12}	3.3×10^{-16}	5.5×10^{-10}	-9.8×10^{-9}	9.8×10^{-9}
3	4.3×10^{-11}	1.5×10^{-15}	1.7×10^{-8}	-4.5×10^{-7}	4.7×10^{-7}
4	-8.1×10^{-12}	7.2×10^{-16}	1.9×10^{-9}	-5.1×10^{-8}	4.7×10^{-8}

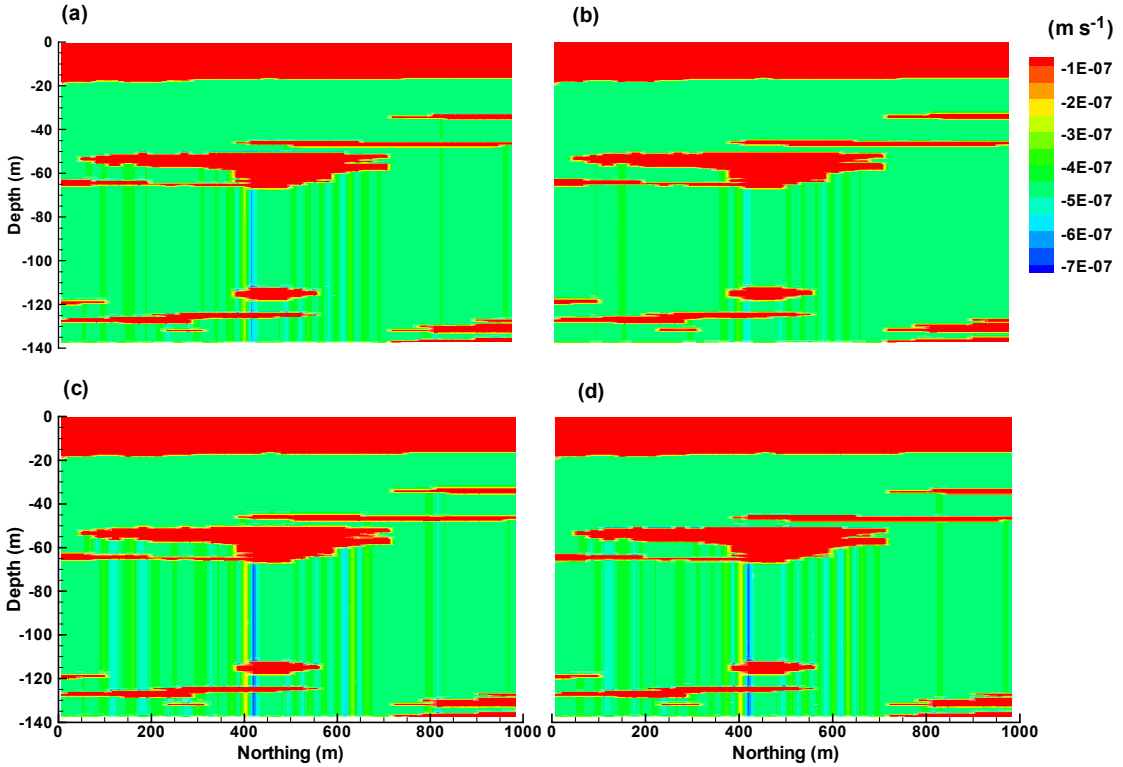

Figure 5. Steady-state vertical pore water velocity for (a) base run, (b) scenario 2, (c) scenario 3, and (d) scenario 4.

Table 6. Steady-state vertical pore-water velocity.

Scenario	Vertical pore-water velocity				
	Mean	Median	SD	Minimum	Maximum
	m s^{-1}				
1 (base run)	-3.4×10^{-7}	-4.6×10^{-7}	2.0×10^{-7}	-8.2×10^{-7}	-7.0×10^{-9}
2	-3.3×10^{-7}	-4.6×10^{-7}	1.9×10^{-7}	-5.7×10^{-7}	-8.0×10^{-9}
3	-3.3×10^{-7}	-4.6×10^{-7}	2.0×10^{-7}	-8.9×10^{-7}	-4.8×10^{-9}
4	-3.3×10^{-7}	-4.6×10^{-7}	2.0×10^{-7}	-8.9×10^{-7}	-5.4×10^{-9}

3.1.4 Water Residence Time

Steady-state water residence time (t) changed from grid block to grid block, and from scenario to scenario (Fig. 6, Table 7). The minimum t values were 4 d for scenarios 1, 3, and 4, and 6 d for scenario 2, while the maximum t values were 1064, 1132, 1533, and 1374 d for scenarios 1–4, respectively. Therefore, the fastest water movement would be slowed down in scenario 2 and the slowest water movement slowed down in scenarios 2–4. Further, the assumption of local equilibrium cation exchange in this study should be adequate for Sr, since cation exchange is very fast between the surface of clay minerals and the solution in contact (McBride, 1994).

The shortest water travel time under steady-state from the SBW leakage to the aquifer differed considerably for different scenarios (Table 8). The travel time was calculated by adding together the steady-state water residence time in each block below the SBW leakage, where the peak concentration of a released contaminant from the SBW would pass through. Scenario 2, with lowest measured permeability assigned to the entirety of all interbeds, led to the longest water travel time of 54.9 yr. Scenario 3, with one-tenth of the lowest measured permeability specified for the top layers of the interbeds, however, resulted in the shortest water travel time through the interbeds (27.4 yr) and the total travel time (43.2 yr), though it led to the longest travel time through the basalts (8.2 yr). Comparing scenario 3 with the base run, water indeed traveled slower (0.24 yr) through the top layers of the interbeds in the former than in the latter (0.09 yr). The shorter travel time through all the interbeds in scenario 3 than in the base run was directly caused by the greater degree of water saturation (0.88–0.98 vs 0.71–0.91) of the low-permeability top layers of the interbeds, since the water saturation for the layers immediately below the top layers was essentially the same (0.71–0.94) in both cases. The higher contrast in water saturation, and thus greater hydraulic gradient, led to $\bar{v}_z$ up to four times higher than in base run through the layers below the surface of the

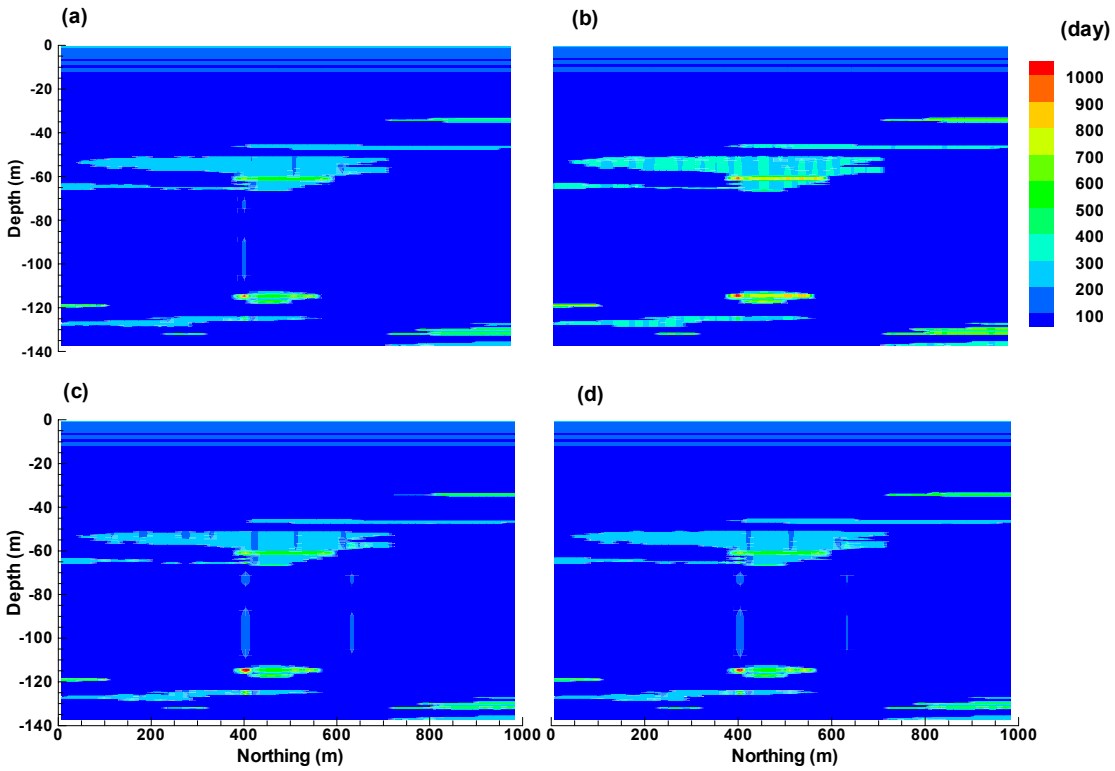

Figure 6. Steady-state water residence time for (a) base run, (b) scenario 2, (c) scenario 3, and (d) scenario 4.

Table 7. Steady-state water residence time.

Scenario	Water residence time				
	Mean	Median	SD	Minimum	Maximum
	d				
1 (base run)	61	15	92	4	1064
2	72	15	116	6	1132
3	60	15	92	4	1533
4	62	15	94	4	1374

Table 8. Steady-state water travel time from sodium-bearing waste (SBW) leakage to groundwater table.

Scenario	Steady-state water travel time			
	Alluvium	Interbeds	Basalts	Total
	yr			
1 (base run)	7.6	28.8	7.7	44.1
2		39.7	7.6	54.9
3		27.4	8.2	43.2
4		29.2	8.0	44.8

interbeds, which in turn led to shorter travel time of 0.45 yr (vs 2 yr in the base run) through all the interbeds.

3.1.5 Uncertainty of Model Inputs on Water Flow

To assess the validity of the assumption of no-flow boundary on both left and right sides, an additional simulation was conducted by assuming a 10^5 times greater vertical permeability for grid blocks along the left side boundary, and a constant water saturation of 0.96 along the right side boundary, with other parameterization kept the same as in the base run. The resultant steady-state water-flow contour (Fig. E.1, Appendix E) was nearly the same as from the base run with dominant vertical movement except at areas along and close to the side boundaries.

The recharge rate of the top boundary, however, might have more complex effect on water flow. Consisting of precipitation, snow melt, Big Lost River infiltration, and anthropogenic sources, the recharge rate may not be constant with time. The variation of flux may affect water flow through the alluvium, and the alluvium may undergo wetting or draining depending on the net flux. How much it would affect water flow in the interbeds and the underlying basalts remained unknown.

Uncertainties affecting water flow results may also exist in the spatial extent of the interbeds, initial water flow condition, temperature, hysteresis of unsaturated water flow, and hydraulic properties of the simulated materials.

3.2 Strontium Transport

3.2.1 Mass Balance

For all four scenarios, it was predicted that the Sr ions from SBW leakage were quickly absorbed by the surrounding matrix. After 2.56 yr, 1.56 yr since SBW leakage, the amount of Sr on exchange sites started to exceed 50% of the total Sr remaining within the model domain (Fig. 7). The amount of total Sr transported to the ground-water aquifer remained low throughout the 200 yr of simulation

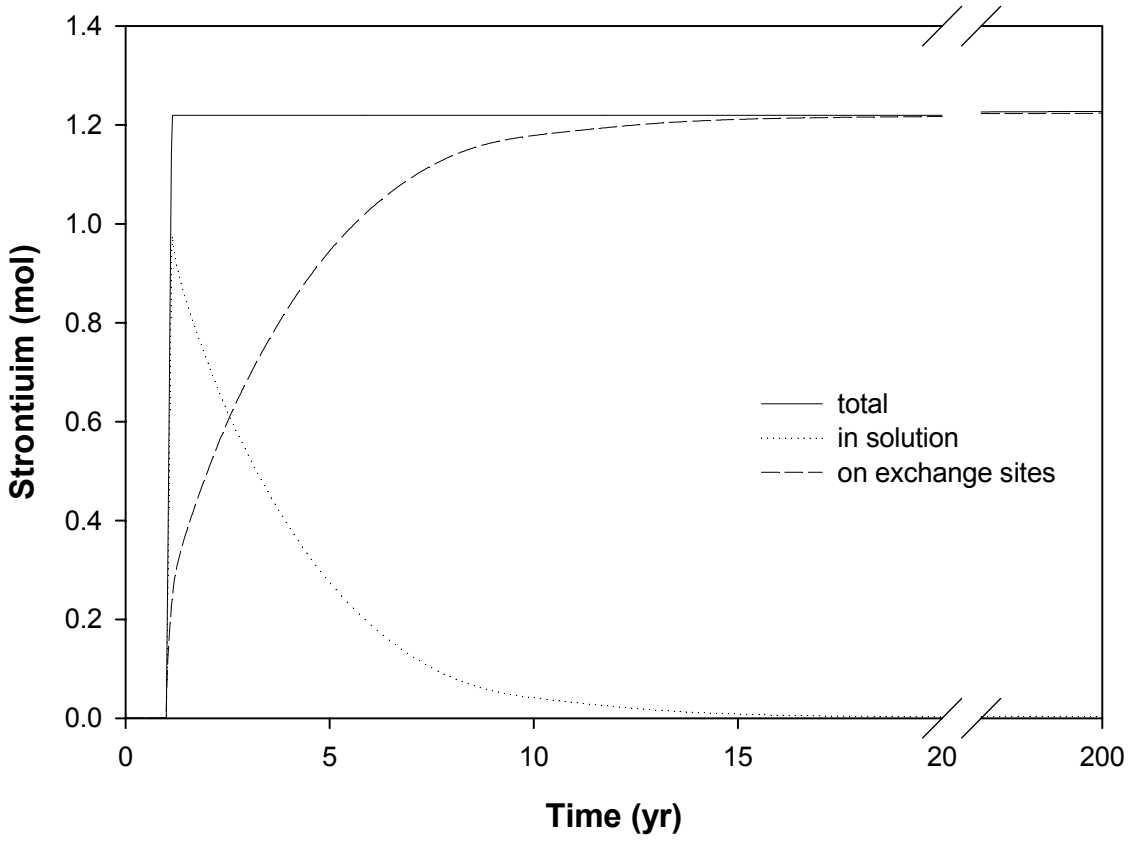

Figure 7. Change in strontium mass distribution with time for base run.

time, amounting to ~5.00×10^{-5} % of the total Sr input, with ~99.7% retained on exchange sites (Table 9), ~0.3% remaining in solution, and ~96.1% (1.177 mol) still in the alluvium.

3.2.2 Strontium Concentration in Solution and on Exchange Sites

3.2.2.1 Aqueous species

Concentrations of the aqueous Sr species, Sr^{2+}, $SrCO_3(aq)$, $SrNO_3^+$, and $SrOH^+$, changed with depth and time (Fig. 8). Near the source and at the beginning of the SBW leakage, the concentration of $SrNO_3^+$ was close to or slightly higher than that of Sr^{2+} because the SBW contained high concentration of NO_3^-. For most of the other time, Sr^{2+} was the dominant species of Sr.

All the Sr species behaved similarly with time, except $SrCO_3(aq)$. At the beginning of SBW leakage and when the peak of NO_3^- reached the ground-water aquifer, all Sr species exhibited a peak at about the same time except $SrCO_3(aq)$ (Fig. 8).

Since the free Sr^{2+} ion was the dominant Sr species and the only Sr species participating in the cation exchange reaction, the presentation and analysis of the results will be focused on Sr^{2+} hereafter.

3.2.2.2 Concentration differences under different mechanisms for perched-water formation

Strontium concentrations during the 200 yr of simulation in the four scenarios were rather similar except in scenario 2. The slower downward movement of a small fraction of Sr in scenario 2 was due to the longer time of travel through the interbeds of low permeability (Fig. 9 and 10). After the small peak, both Sr ion concentrations in solution (Sr^{2+}) and on exchange sites (SrX_2) near the ground-water table were higher in scenario 2 than in other three scenarios.

For the areas of high concentration (Fig. 9), the differences were negligible throughout the 200 yr of simulation. For example, the maximum Sr^{2+} concentrations in solution after 50 yr were 7.023×10^{-9} and 7.017×10^{-9} mol L^{-1} for base run and scenario 2, respectively, and both were at the

Table 9. Mass balance of strontium transport after ~200 years of simulation.

Scenario	Input	Output	Initial aqueous state	Initial solid state	Ending aqueous state	Ending solid state	Mass balance error
	mol						%
1(base run)	1.227	6.142×10^{-7}	1.537×10^{-7}	3.294×10^{-5}	3.546×10^{-3}	1.224	0.02
2		6.148×10^{-7}	1.802×10^{-7}	3.208×10^{-5}	3.560×10^{-3}	1.224	0.01
3		6.140×10^{-7}	1.499×10^{-7}	3.397×10^{-5}	3.530×10^{-3}	1.224	0.02
4		6.140×10^{-7}	1.548×10^{-7}	3.294×10^{-5}	3.544×10^{-3}	1.223	0.04

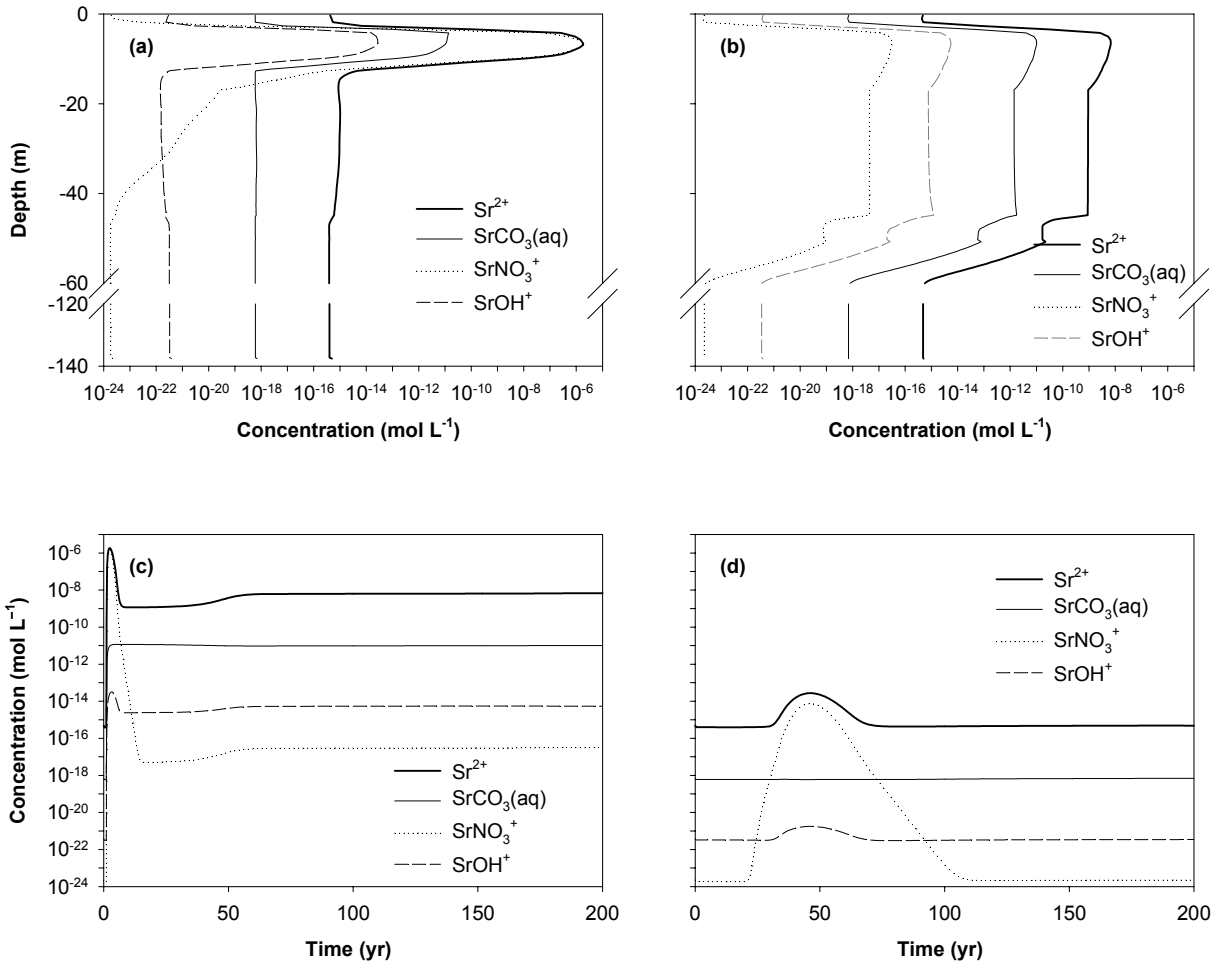

Figure 8. Change in concentration of strontium species (a) with depth at 2.5 yr, (b) with depth at 200 yr, (c) with time at Obs. 1, and (d) with time at Obs. 4.

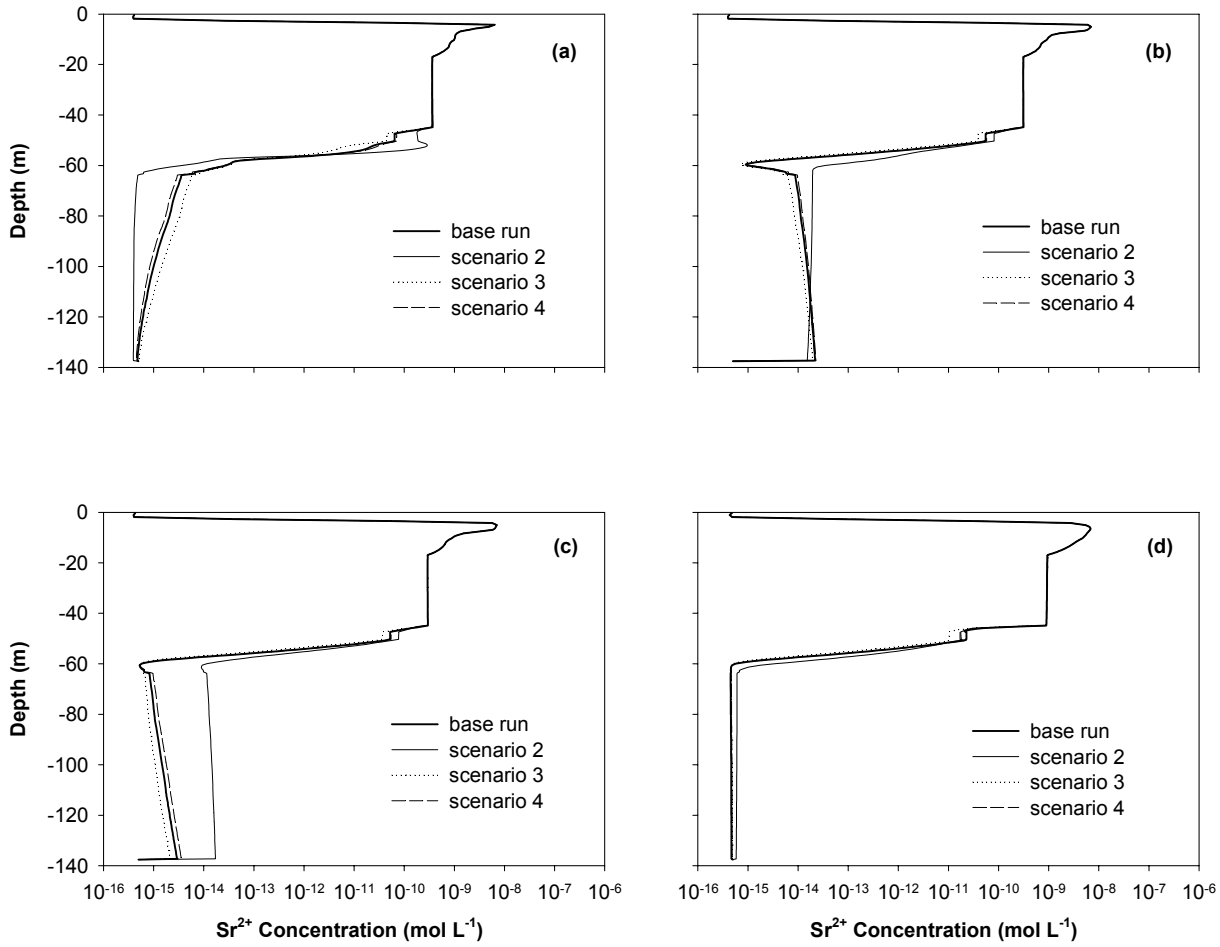

Figure 9. Difference of strontium concentration between scenarios at (a) 30 yr, (b) 50 yr, (c) 60 yr, and (d) 200 yr.

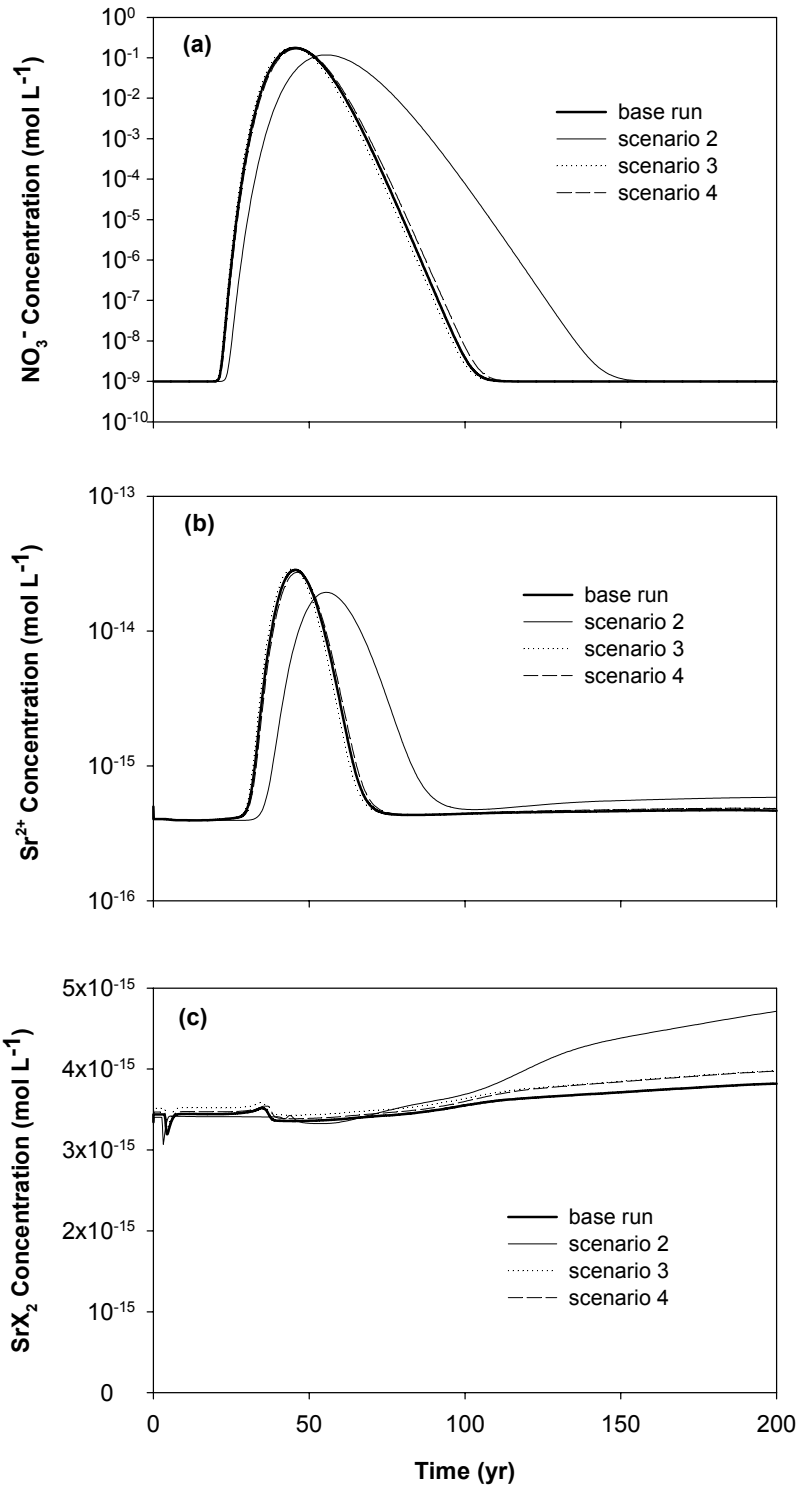

Figure 10. Effects of different mechanisms of perched water formation on concentration of (a) NO_3^-, (b) Sr^{2+}, and (c) SrX_2 change with time at Obs. 4.

depth of 5.048 m; the maximum SrX_2 concentrations on exchange sites occurred at the same depth, at 2.602×10^{-6} mol L^{-1} for base run vs. 2.601×10^{-6} mol L^{-1} for scenario 2. After 200 yr, the maximum concentrations occurred at the depth of 6.553 m, only 1.5 m further down, with Sr^{2+} concentration of 6.848×10^{-9} mol L^{-1} and SrX_2 concentration of 2.454×10^{-6} mol L^{-1} for base run, and Sr^{2+} concentration of 6.847×10^{-9} mol L^{-1} and SrX_2 concentration of 2.452×10^{-6} mol L^{-1} for scenario 2.

Differences in Sr^{2+} and SrX_2 concentration profiles under different mechanisms for perched-water formation—excluding scenario 2—appeared minor during the 200 yr of simulation. This outcome was likely due to the retardation of Sr transport by cation exchange. By the end of the simulation time, the peak concentration of Sr has not moved beyond the interbeds, and therefore the differences caused by the different mechanisms for perched-water formation have not manifested However, over a long term, the differences may be substantial, especially by considering scenario 2, which already led to different characteristics of Sr transport compared to others within 200 yr. The insignificant differences of Sr transport between the other three scenarios was consistent with water flow, especially water travel time. For clarity, only Sr transport for base run will be presented hereafter, when other scenarios had similar results.

3.2.2.3 Change in concentration with depth and time

Strontium transported downwards with water movement. The bulk of Sr was retarded by cation exchange reactions in alluvium and interbeds. A small fraction, however, passed through the interbed barrier. This small fraction of Sr, accounting for only 1.4×10^{-5}% of the total Sr input, moved out of the interbed together with the center region of NO_3^- plume. The concentration peak of this small fraction reached the ground-water table in ~45 yr of simulation (Fig. 10b). This rapidly moving plume indicates a low distribution coefficient (K_d) for Sr^{2+}. The low K_d, accompanying the plume of NO_3^-, was a result of (i) competition for exchange sites by Na^+ from the waste solution and Ca^{2+}

released by dissolution of calcite, and (ii) complexing with NO_3^-. Once the waste plume had passed, the residual Sr was not particularly mobile (Fig. 11, 12) because Sr has a lower selectivity coefficient (more strongly to compete) for exchange sites than Na or Ca.

The small mobile fraction of Sr reached the aquifer in 45 years. This is too fast for radioactive decay to remove much of the activity of Sr-90, which has a half life of 29.1 yr, and so the existence of this mobile fraction may be significant for risk assessment. The peak concentration of the small Sr^{2+} plume was 2.84×10^{-14} mol L^{-1}, corresponding to Sr-90 peak concentration of 350 pCi L^{-1}, and the steady-state water flux was 0.162 m yr^{-1} (Darcy velocity). Assuming that the Sr-90 plume instantaneously mix with a depth of 15 m, Darcy velocity of 21.9 m yr^{-1}, southward flowing ground water (Cahn et al., 2006), the peak Sr-90 concentration in aquifer resulted by this plume would be 2.6 pCi L^{-1}. Though this value was lower than the Maximum Contaminant Level (MCL) of 8 pCi L^{-1}, risk for contamination to the aquifer may still exist because of the uncertainty of model inputs. A small decrease of the interbed depth or CEC might result in a big increase of the peak concentration of this small plume. Uncertainty of interbed depth, recharge rate, and preferential flow may also indicate variation of time for this small plume reaching the ground-water table.

From the results of the base run, the peak of NO_3^- concentration reached the ground-water aquifer 44 yr after the SBW leakage (Table 8, Fig. 10a, 12). The peak concentration of Sr^{2+} was retarded mostly due to cation exchange in the alluvium and interbeds at the top 60 m. Both Sr^{2+} concentration in solution and SrX_2 concentration on exchange sites remained high in these regions, even after 200 yr (Fig. 12). The peak Sr^{2+} concentration after 5 yr was 7.676×10^{-7} mol L^{-1}, at the depth of 10.27 m; and peak SrX_2 concentration at this time was 2.71×10^{-6} mol L^{-1}, still at the SBW source. With slowly moving downward, the SrX_2 concentration in areas that were in front of the SrX_2 peak kept increasing, until became the new peak (Fig. 12); while the Sr^{2+} concentration peak

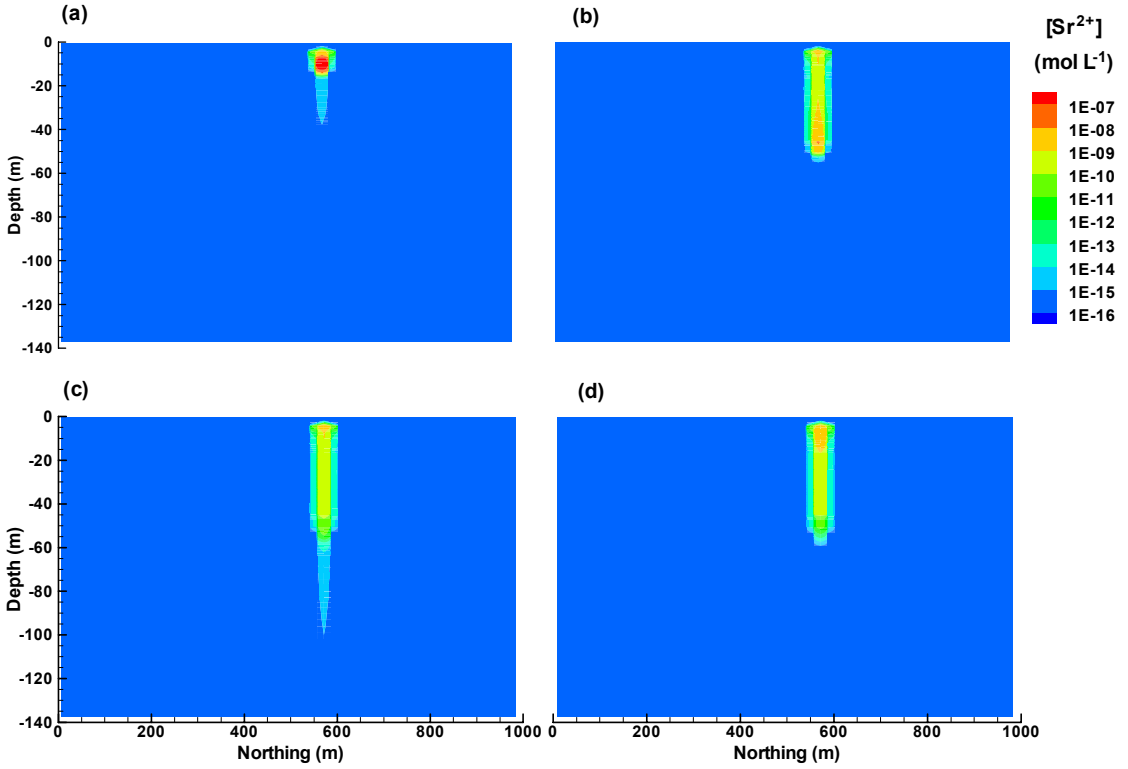

Figure 11. Strontium ion concentration for base run at (a) 5 yr, (b) 15 yr, (c) 30 yr, and (d) 200 yr.

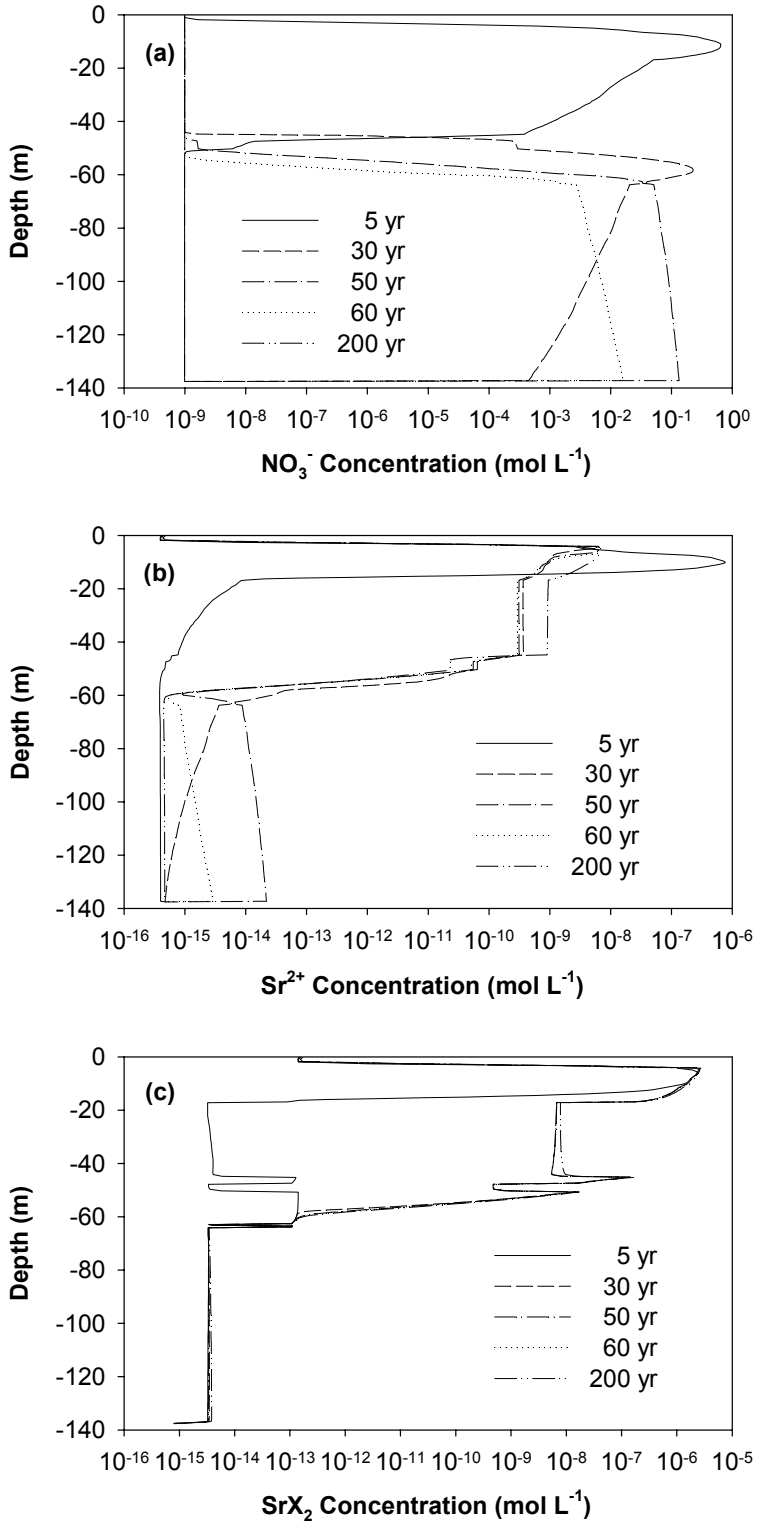

Figure 12. Concentration of (a) NO_3^-, (b) Sr^{2+}, and (c) SrX_2 with depth for base run.

was quickly absorbed by exchange sites via cation exchange reaction. After 200 yr, the highest Sr^{2+} and SrX_2 concentrations were found at the depth of 6.553 m, with Sr^{2+} concentration of 6.848×10^{-9} mol L^{-1} and SrX_2 concentration of 2.454×10^{-6} mol L^{-1}. After 5 yr, the SrX_2 concentration became much higher than that of the Sr^{2+} between the SBW source and depth of 50 m (Fig. 12).

3.2.2.4 Changes in concentrations at the observation points

During the 200 yr of simulation, concentration of Sr^{2+} was highest in alluvium (Obs. 1) and lowest before entering ground-water aquifer (Obs. 4) for most of the time (Fig. 13). The differences between the uppermost basalt (Obs. 2) and the uppermost interbed (Obs. 3) were less significant, meaning that a region with relatively constant Sr^{2+} concentration existed between the alluvium and the first layer on interbed beneath SBW leakage (Fig. 12b, 13a). After its first peak, concentrations of Sr^{2+} dropped a few orders of magnitude, varying with depth. The second Sr^{2+} concentration rise started to migrate passing Obs. 1–3, though the peak had not occurred until the end of the 200 yr of simulation.

The concentration of SrX_2 on the exchange sites was higher in alluvium and interbeds than in basalts throughout the 200 yr of simulation (Fig. 13b). Though the interbeds had higher CEC than the alluvium, the SrX_2 concentration was still lower in the interbeds (Obs. 3) than in the alluvium (Obs. 1) because the peak concentrations of Sr^{2+} and SrX_2 remained in the alluvium (Fig. 12).

Within the simulated 200 yr, cation exchange curves for Obs. 1–3 showed continuous sorbing for Sr^{2+} by exchange sites, even when the first main peak was passing (Fig. 14), indicating that SrX_2 concentrations had not reach their peak values for these points. For Obs. 4, however, a ten-yr desorbing was noticed between 35–45 yr, till the small Sr^{2+} peak passed (Fig. 13a). The SrX_2 concentration on exchange sites of Obs. 4 was very small, ranging 1.6×10^{-17}–1.8×10^{-17} mol kg^{-1} solid, and its change could not be noticed in Fig. 13b.

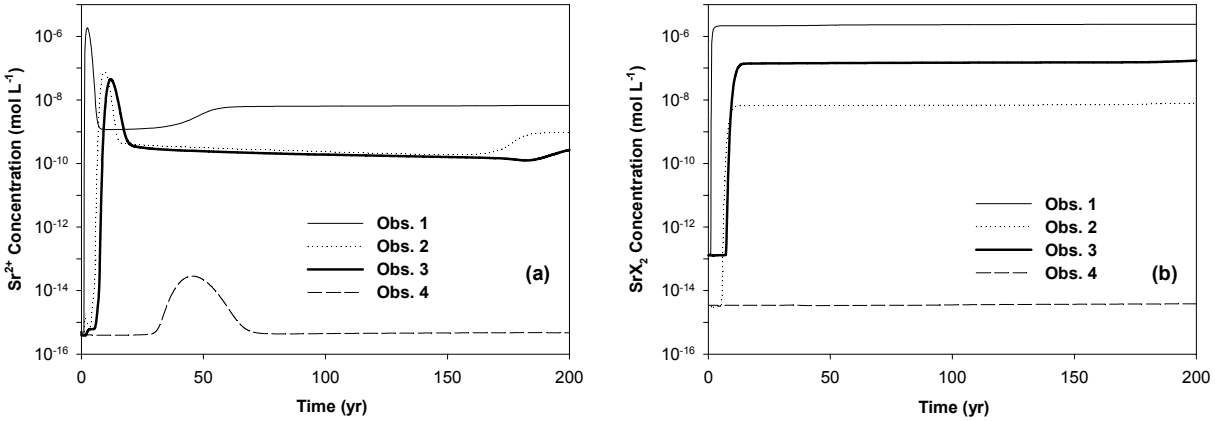

Figure 13. Concentration of (a) Sr^{2+} and (b) SrX_2 with time at Obs. 1–4 for base run.

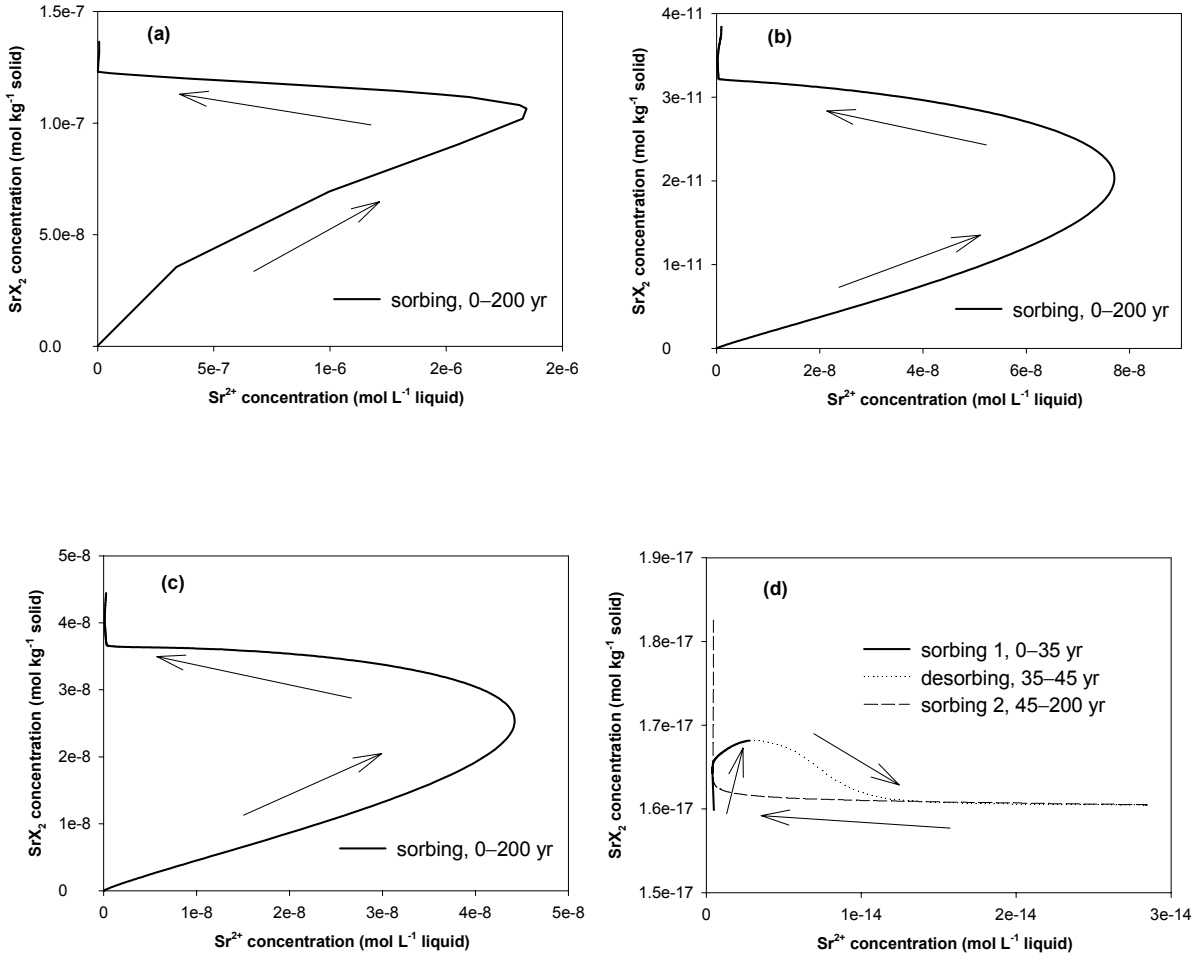

Figure 14. Cation exchange curves within 200 yr for (a) Obs. 1, (b) Obs. 2, (c) Obs. 3, and (d) Obs. 4.

3.2.3 Mineral dissolution and precipitation

The initial calcite volume fraction was 0.05. Since the SBW contained 1.5 mol L^{-1} HNO_3, part of calcite was dissolved at and near the SBW leakage, releasing Ca^{2+} into solution. The released Ca^{2+}, competed with Na^+ and Sr^{2+} for the exchange sites. When recharge water, containing higher concentration of Ca^{2+} than Na^+, came into the system, Ca^{2+} would further displace Na^+ from exchange sites and removing Ca^{2+} from solution, causing more dissolution of calcite, the resultant mineral fraction at Obs. 1 changed from 0.0340 (initial fraction of 0.05 for solid with porosity of 0.32 for Obs. 1 in alluvium) to 0.0338 (Fig. 15a).

As the high concentration of Na^+ plume migrated further downward, Na^+ displaced Ca^{2+} from exchange sites, resulting in precipitation of calcite. At Obs. 3, calcite total volume fraction changed from 0.0265 (0.05 solid volume fraction with porosity of 0.47 for Obs. 3 in interbed) to 0.0269 at ~170 yr of simulation along with the increasing concentration of Na^+, and then dropped back to 0.0266 because of the deceasing Na^+ (Fig. 15b).

Since Sr^{2+} can exchange with Ca^{2+} in sites at the surface of calcite (Parkman et al., 1998), the dissolution of calcite would result in decreased CEC of the medium, and the precipitation of calcite would result in increased CEC. Since CEC was considered constant for a material in the model, when there was calcite dissolution, the model would under-estimate Sr^{2+} transport rate; when there was calcite precipitation, the model would over-estimate Sr transport rate, though the effect was very small due to the small fraction of calcite dissolution and precipitation.

Initially, there was no gibbsite in the system. Since the SBW contained high concentration of Al^{3+} and NO_3^-, precipitation of gibbsite occurred with the plume of Al^{3+} and the neutralizing of NO_3^- at shallower depth. At Obs. 1, total volume fraction of gibbsite increased to 6×10^{-10} and dropped back to 0 after 33 yr of simulation (Fig. 15c). As the high concentration of Na^+ plume migrated further

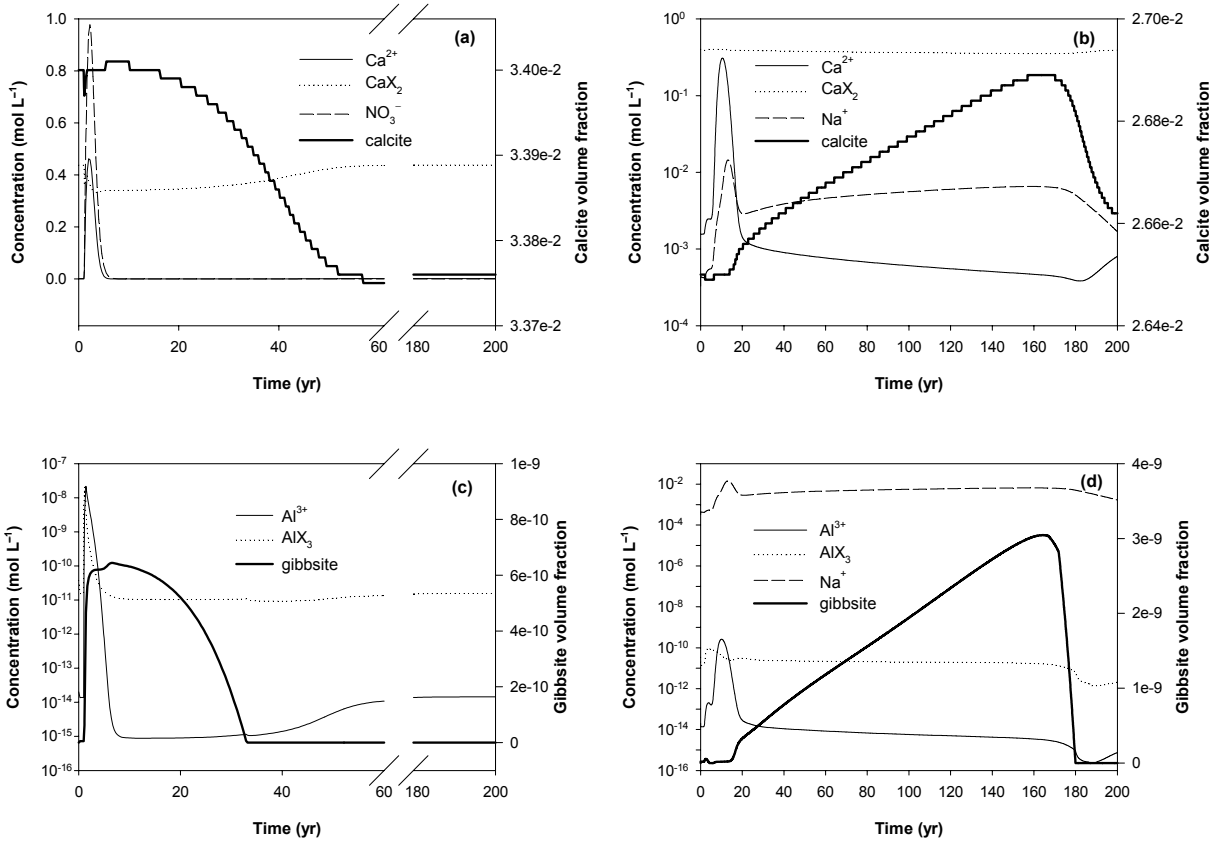

Figure 15. Mineral dissolution and precipitation. (a) calcite at Obs. 1, (b) calcite at Obs. 3, (c) gibbsite at Obs. 1, and (d) gibbsite at Obs. 3.

downward, Na^+ also displaced Al^{3+} from exchange sites, resulting in more precipitation of gibbsite. Total volume fraction of gibbsite at Obs. 3 increased to 3×10^{-9} along with increasing concentration of Na^+, and then dissolved after 170 yr of simulation time, with the decreasing Na^+ concentration (Fig. 15d). Since the resultant gibbsite fraction was very small, the effect on CEC change was negligible.

3.2.4 Distribution Coefficient and Retardation Factor for Strontium

Not only K_d and R_f changed with material, they also changed with time, when concentrations of Sr^{2+}, SrX_2 and other competing ions changed (Fig. 16, F.1, F.2). This was consistent with Hemming et al. (1997), Bunde et al. (1998), Zhu and Anderson (2002), and many other studies. For the base run, K_d ranged 0.05–105 L kg^{-1} for the alluvium, 0.4–323 L kg^{-1} for interbeds, and was less than 0.2 L kg^{-1} for basalts. The retardation factor for Sr^{2+} ranged 2–1866 for the alluvium, 2–1244 for the interbeds, and 1–38 for basalts. Since the largest change in concentration occurred below the SBW leakage, K_d and R_f for this region changed the most, and remained relatively constant within the same material in regions horizontally away from the SBW leakage.

For each observation point, there was a decrease of K_d for Sr^{2+} over time (Fig. 16a), followed by an increase and then decrease again to the original value. In addition to the change in the concentration of Sr^{2+} in solution and on exchange sites, the concentration of other cations also contributed to the change in K_d. The first decrease of K_d was mainly because of the increased total concentration of cations in solution competing for the exchange sites (Fig. 17). When the SBW plume passed through, Na^+ in solution displaced lots of Ca^{2+} from exchange sites. This resulted in the increase of K_d for Sr^{2+}, since Sr^{2+} could more easily displace Na^+ than it could displace Ca^{2+}. After the Na^+ concentration peak, Ca^{2+} from recharge water could easily displace Na^+ from exchange sites, resulting in decreased K_d for Sr^{2+}, until K_d dropped to the original value.

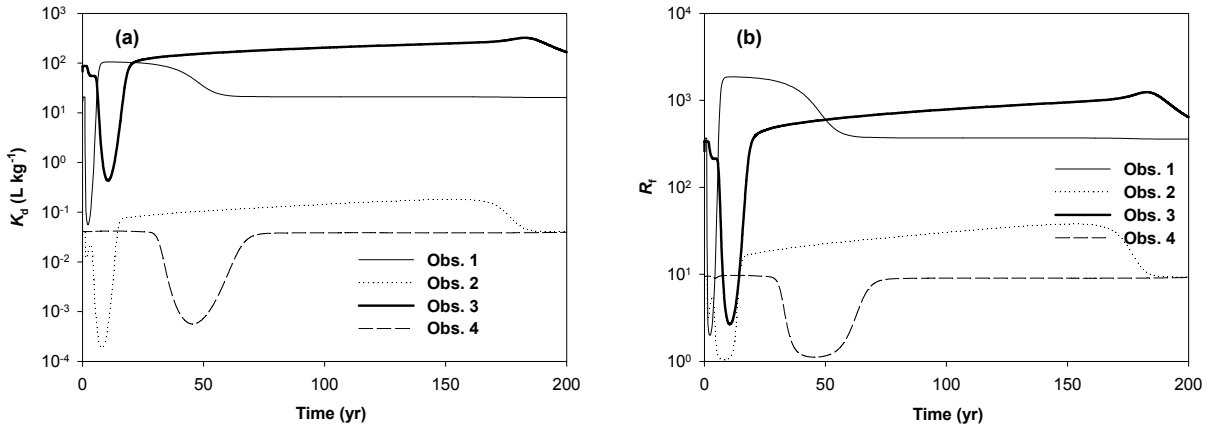

Figure 16. (a) Distribution coefficient and (b) retardation factor for strontium with time at Obs. 1–4 for base run.

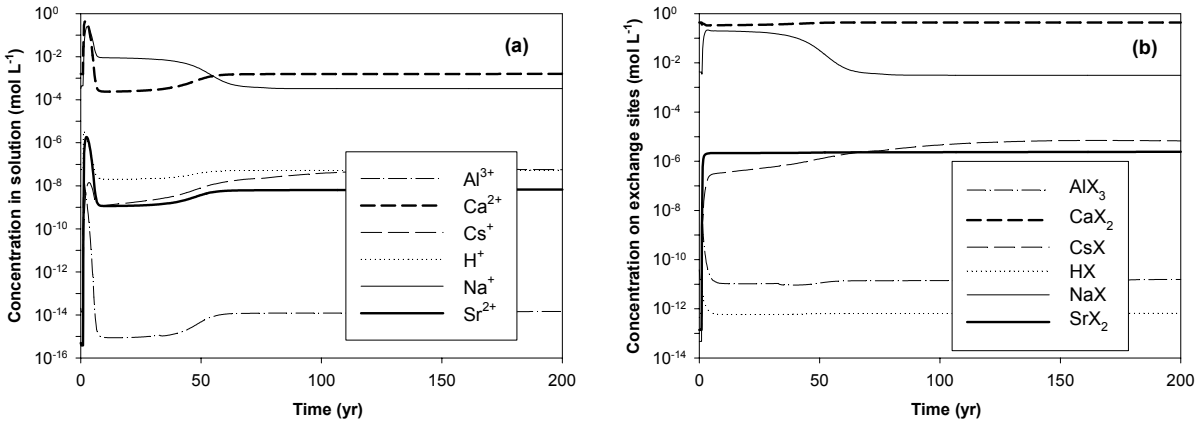

Figure 17. Cation concentration (a) in solution and (b) on exchange sites with time at Obs. 1 for base run.

3.2.5 Uncertainty of Model Inputs on Strontium Transport

Obviously, the factors that affect water flow will also affect Sr transport. In addition, uncertainties existed in defining the initial- and boundary-water composition, SBW volume, CEC values of the simulated material, diffusion coefficient, and geochemical processes. Because of the existence of so many uncertainties, the results presented here should be used with care.

CHAPTER FOUR

SUMMARY AND CONCLUSIONS

Idaho Nuclear Technology and Engineering Center (INTEC) is a major facility of Idaho National Laboratory (INL) located in the Snake River Plain near Idaho Falls, Idaho, USA. Built in the early 1950s, the INTEC has been used to receive, store, and process legacy nuclear wastes. An accidental release of 70 m^3 of sodium-bearing waste (SBW) at the INTEC in 1972 has raised serious public concerns over ground-water contamination.

A *2*-dimensional simulation using TOUGHREACT was conducted to investigate Sr-90 transport in variably-saturated, heterogeneous subsurface at the INTEC, INL, Idaho, USA. Three different mechanisms for perched-water formation, including low permeability of interbed, "baked" surfaces, infilling of fractures, were examined for their impact on water flow and Sr transport in INTEC's subsurface comprising an alluvium layer near the land surface, multiple basalt layers and sediment interbeds, comparing with base run. These mechanisms were simulated by four scenarios: scenario 1 (base run), with the geometric mean of field-measured interbed permeability, 2.18×10^{-13} m^2, assumed for all interbeds; scenario 2, with the smallest field-measured interbed permeability, 3.00×10^{-13} m^2, assumed for all interbeds; scenario 3, with one tenth of the smallest field-measured interbed permeability assumed for the top layer of interbeds at depths of 20–85 m; and scenario 4, with the smallest field-measured interbed permeability assumed for the top layer of basaltic rocks underlying interbeds at depths of 20–85 m. The accidental SBW leakage, which contained high concentration of Sr-90, was simulated as the source term.

The results showed that different mechanisms led to different saturated zones inside or near the interbeds: they were mainly saturated near their interfaces with the underlying basaltic rocks in the base run and scenario 4, were nearly completely saturated in scenario 2; and were saturated at their

interfaces with both underlying and overlying basaltic rocks in scenario 3. Though water flow was vertically dominant for all scenarios, the ranges of horizontal and vertical pore-water velocities, water residence time, and water travel time from the SBW leakage to ground-water table all varied under different mechanisms of perched-water formation. Scenario 2 led to longest water travel time, while scenario 3 resulted longest water residence time.

In the 200 yr of simulation, the Sr^{2+} and SrX_2 concentrations profiles and their changes with time showed minor differences among scenarios 1, 3 and 4. Scenario 2, with the longest water travel time, delayed the arrival of the first concentration peak of Sr^{2+} for about 10 yr. However, the higher concentration of Sr^{2+} reaching the ground-water table after this peak resulted slightly faster Sr transport to the aquifer. The total Sr mass balance was nearly the same for all four scenarios, with a small fraction transported to the ground-water aquifer by the end of 200 yr, 99.7% remaining on the exchange sites, and 96.1% remaining within the alluvium. Two areas of high Sr^{2+} concentrations were found at different depths beneath the SBW leakage at ~15 yr. A small fraction of Sr plume arrived at ground-water table in ~45 yr of simulation. After 200 yr, the highest Sr^{2+} concentration was 6.85×10^{-9} mol L^{-1} and highest SrX_2 concentration was 2.45×10^{-6} mol L^{-1}, both at the depth of 6.55 m, still inside the alluvium. The distribution coefficient and retardation factor for Sr^{2+} changed more than one order of magnitude for the same material with time, which is a consequence of varying concentrations of Sr^{2+} in solution, SrX_2 on exchange sites as well as other competing ions.

These results indicate that a small Sr plume was quickly moving toward the aquifer, and under regular environmental, hydrological, and geochemical conditions, the migration of the bulk of Sr-90 toward the ground-water aquifer would be limited at relatively shallower depths for a long time. Decrease of observed Sr-90 concentration in perched-water might be followed by anther increase.

Monitoring strategy, combining with model calibration and parameterization, is crucial in order to determine the change of Sr-90 concentration on exchange sites with the least perturbation.

REFERENCES

Appelo, C. A. J. and D. Postma. 1996. Geochemistry, Groundwater, and Pollution. A. A. Balkema Publishers, Rotterdam, Netherlands.

Bascetin, E., and G. Atun. 2006. Adsorption behavior of strontium on binary mineral mixtures of Montmorillonite and Kaolinite. Appl. Radiat. Isot. 64:957–964.

Bilgin, B., G. Atun, and G. Keçeli. 2001. Adsorption of strontium on illite. J. Radioanal. Nucl. Chem. 250:323–328.

Bunde, R.L., J.J. Rosentreter, M.J. Liszewski. 1998. Rate of strontium sorption and the effects of variable aqueous concentrations of sodium and potassium on strontium distribution coefficients of a surficial sediment at the Idaho National Engineering Laboratory, Idaho. Environ. Geol. 34:135–142.

Cahn, L.S., M. L. Abbott, J.F. Keck, P. Martian, A.L. Schafer, and M.C. Swenson. 2006. Operable Unit 3-14 Tank Farm Soil and Groundwater Remedial Investigation/Baseline Risk Assessment. DOE/NE-ID-11227, Revision 0, Project No. 23512. Prepared for the US DOE Idaho Oper. Off., Idaho Falls, ID.

Cecil, L.D., B.R. Orr, T. Norton, and S.R. Anderson. 1991. Formation of perched ground-water zones and concentrations of selected chemical constituents in water, Idaho Natl. Eng. Lab., Idaho, 1986–88. USGS Water Resour. Invest. Rep.91-4166 (DOE/ID-22100). USGS, Idaho Falls, ID.

Hemming, C.H., R.L. Bunde, M.J. Lizewski, J.J. Rosentreter and J. Welhan. 1997. Effect of experimental technique on the determination of strontium distribution coefficients of a superficial sediment from the Idaho National Engineering Laboratory, Idaho, Water Res. 31:1629–1636.

Hull, L.C., C.W. Bishop, J.R. Giles, T.S. Green, D.J. Haley, K.N. Keck, S.O. Magnuson, P. Martian, K.D., McAllister, J.M. McCarthy, A.S. Wood, and P.A. Tucker, 1999. Draft Work Plan for the Waste Area, Group 3, Operable Unit 3-14, Tank Farm Soil and Groundwater, Remedial Investigation/Feasibility Study, DOE/ID-10676, Rev. 2, Lockheed Martin Idaho Technologies Company, Idaho Falls, ID.

Hull, L.C., and A.L. Schafer. 2005. OU 3-14 Tank Farm Alluvium Geochemical Properties Report. DOE/ID-11271, Revision 0, Project No. 23512. Prepared for the US DOE Idaho Oper. Off., Idaho Falls, ID.

Ludwig, B., F. Beese, and K. Michel. 2005. Modeling cation transport and pH buffering during unsaturated flow through intact subsoils. Eur. J. Soil Sci. 56:635–645

MacQuarrie, K.T.B., and K.U. Mayer. 2005. Reactive transport modeling in fractured rock: A state-of-the-science review. Earth Sci. Rev. 72:189–227.

Magnuson, S.O., 1995, Inverse Modeling for Field-Scale Hydrologic and Transport Parameters of Fractured Basalt, INEL-95/0637, Idaho Natl. Eng. Lab., Idaho Falls, ID.

Magnuson, S.O. 2004. Regulatory modeling for the Idaho National Engineering and Environmental Laboratory's Subsurface Disposal Area and conceptual model uncertainty treatment. Vadose Zone J. 3:59–74.

Mattson, E.D., S.O. Magnuson, and S.L. Ansley. 2004. Interpreting INEEL vadose zone water movement on the basis of large-scale field tests and long-term vadose zone monitoring results. Vadose Zone J. 3:35–46.

McBride, M.B. 1994. Environmental Chemistry of Soils. Oxford University Press, New York.

Nimmo, J.R., J.P. Rousseau, K. S. Perkins, K.G. Stollenwerk, P.D. Glynn, R.C. Bartholomay, and L.L. Knobel. 2004. Hydraulic and geochemical framework of the Idaho National Engineering and Environmental Laboratory vadose zone. Vadose Zone J. 3:6–34.

Oreskes, N., K. Shrader-Frechette, and K. Belitz. 1994. Verification, validation, and confirmation of numerical models in the Earth sciences. Science 263:641–646.

Parkman, R.H., J.M. Charnock, F. R. Livens, D. J. Vaughan. 1998. A study of the interaction of strontium ions in aqueous solution with the surfaces of calcite and kaolinite. Geochim. Cosmochim. Acta 62:1481–1492.

Pruess, K., C. Oldenburg, and G. Moridis. 1999. TOUGH2 User's Guide, ver. 2.0. Rep. LBNL-43134. Lawrence Berkeley Natl. Lab., Berkeley, CA.

Rykiel, E.J. 1996. Testing ecological models: the meaning of validation. Ecol. Model. 90:229–244.

Schaap, M.G., and M. Th. van Genuchten. 2006. A modified Mualem–van Genuchten formulation for improved description of the hydraulic conductivity near saturation. Vadose Zone J. 5:27–34.

Schafer, A.L., P. Martian, J.M. McCarthy, and T. Honeycutt. 1997. Comprehensive RI/FS for the Idaho Chemical Processing Plant OU 3-13 at the INEEL, Appendix F: WAG-3 Vadose Zone and Aquifer RI/FS Contaminant Source Identification and Fate and Transport Modeling Results, DOE/ID-10534, US DOE, Idaho Falls, ID.

Spycher, N.F., E.L. Sonnenthal, and J.A. Apps. 2003. Fluid flow and reactive transport around potential nuclear waste emplacement tunnels at Yucca Mountain, Nevada. J. Contam. Hydrol. 62–63:653– 673.

Steefel, C.I., S. Carroll, P. Zhao, and S. Roberts. 2003. Cesium migration in Hanford sediment: a multisite cation exchange model based on laboratory transport experiments. J. Contam. Hydrol.67:219–246.

van Genuchten, M. Th. 1980. A Closed-Form Equation for Predicting the Hydraulic Conductivity of Unsaturated Soils, Soil Sci. Soc. Am. J. 44:892–898.

Welhan, J.A., C.M. Johannesen, K.S. Reeves, T.M. Clemo, J.A. Glover, and K.W. Bosworth. 2002. Morphology of inflated pahoehoe lavas and spatial architecture of their porous and permeable zones, eastern Snake River Plain, Idaho. *In* Link, P.K., and L.L. Mink, eds., Geology, Hydrogeology, and Environmental Remediation: Idaho National Engineering and Environmental Laboratory, Eastern Snake River Plain, Idaho: Boulder, Colorado, Geol. Soc. Am. Spec. Pap. 353:135–150.

Xu, T., and K. Pruess, 2001. Modeling multiphase non-isothermal fluid flow and reactive geochemical transport in variably saturated fractured rocks: 1. Methodology. Am. J. Sci., 301:16–33.

Xu, T., J. Samper, C. Ayora, M. Manzano, and E. Custodio. 1999. Modeling of non-isothermal multi-component reactive transport in field scale porous media flow systems. J. Hydrol. 214:144–164.

Xu, T., E. Sonnenthal, N. Spycher, and K. Pruess, 2004. TOUGHREACT User's Guide: A Simulation Program for Non-isothermal Multiphase Reactive Geochemical Transport in Variable Saturated Geologic Media. Lawrence Berkeley Natl. Lab. Rep. LBNL-55460, Berkeley, CA.

Yang, L., 2005. Stochastic Modeling of Water Flow Through a Variably-saturated, Heterogeneous Field at Idaho National Laboratory: Uncertainty Analysis. MS thesis. Washington State Univ., Pullman, WA.

Zhu, C., and G. Anderson. 2002. Environmental Applications of Geochemical Modeling. Cambridge University Press, London.

Zhu, C., 2003. A case against K-d based transport models: natural attenuation at a mill tailings site. Comput. Geosci. 29:351–359.

APPENDIX

A. UTILITY CODES

A.1. Converting output file of EOS9 flow system to input file for EOS3 flow system

```
   program SAVE_INCON
!
!     Write output "SAVE" from module EOS9 to "INCON" used by module EOS3. L. Wang, 06/06/2006.
!     Add option to set saturated zones to prevent air from being trapped above low-permeability materials.
!     If simulation starts from gravity-capillary equilibrium condition, air may be traped by downward water flow
!     when flux was added   at the top boundary (Jerry Fairley, personal communication, 02/27/2007). L. Wang,
03/02/2007.
!
      implicit none
      integer::eleme, i, n_sz, j, NEOS
      real(8)::X1, X2, X3, PORX, PERX, PERY, PERZ, XX2, PSAT
      REAL(8)::MAT, NAD, DROK, POR, PER(3), CWET, SPHT, SL, SG, TEMP, PRES
      real(8)::xmin(100), xmax(100), zmin(100), zmax(100)
      real(8)::volx, ahtx, pmx, x(100000), y, z(100000)
      real(8)::zi, xi, xc, SLz, SLx, SL0
      character::EL*3, WORD*5, MA1*3, MA2*2, NE*2, NSEQ*5, NADD*5
      character::atitle1*31, atitle2*33, atime_step*45, yn_sz*1
!
!     For initial air pressure PA=1.013e+5, the calculated air fraction is
!     XX(2)=1.6283469960d-5.
!     For water vapor, PSAT = 0.316599e+4 Pa at 25C.
!     XX2 = 1.6283469960d-5
!     To maintain Pg=1.013e+5, it needs Pa=1.013e+5-Psat=1.013e+5-0.0316599e+05=0.9813401e+05.
!     The calculated air fraction is XX(2) = 1.57745558840168e-05
!     XX2 = 1.57745558840168d-05       ! Converges very slow when add the REACT part back.
      PSAT = 0.316599d+4
      PRES = 1.013d+05
!     Since the program converges very slow when using the single phase for the BOUND,
!     change the single phase to two-phase with a very small SG by setting SG = 1.0e-07.
      XX2 = 1.0d+01 + 1.0d-07
      write(*,*)'Perform SAVE ---> INCON file exchange'
      write(*,121)
      read(*,*) NEOS
      if(NEOS /= 2) NEOS = 1
      write(*,*)'Set saturated zones (Y/N)? [Y]'
      read(*,*) yn_sz
      if(yn_sz /= 'N' .and. yn_sz /= 'n') yn_sz = 'Y'
!
      open(3, file='flow.inp', status='old')
10    read(3, '(a5)') WORD
      if(WORD /= 'ROCKS') goto 10
20        read(3, 111) MAT, NAD, DROK, POR, (PER(I), I=1,3), CWET, SPHT
          if(MAT == 'REFCO') then
!             ZREF = CWET
!             PRES = (ZREF + 137.6164d0 + 0.3166d0) * 1.0d+04
              PRES = DROK
          elseif(MAT /= '     ') then
              goto 20
          endif
!
      if(yn_sz == 'Y') then
```

```
          open(6, file='sz.inp', status='old')
          read(6, *) n_sz, SL0
          do j = 1, n_sz
               read(6, *) xmin(j), xmax(j), zmin(j), zmax(j)
          enddo
          close(6)
!
          I = 1
30      read(3, '(a5)') WORD
          if(WORD /= 'ELEME') goto 30
40           read(3, 112) EL, NE, NSEQ, NADD, MA1, MA2, VOLX, &
                  AHTX, PMX, X(I), Y, Z(I)
               I = I + 1
               IF(EL /= '   ') GOTO 40
   endif
     I = I - 1
     close(3)

     open(1, file='save', status='old')
     open(2, file='incon', status='unknown')
     read(1, 100) atitle1, eleme, atitle2
!    IF(I /= ELEME) THEN
!         WRITE(*,*) 'Element number does not match!'
!         WRITE(*,*) 'Skip setting of saturated zone!'
!         PAUSE
!         GOTO 999
!    ENDIF
     write(2, 100) atitle1, eleme, atitle2

     do i=1, eleme
          read(1, 101) EL, NE, NSEQ, NADD, PORX, PERX, PERY, PERZ
          write(2, 101) EL, NE, NSEQ, NADD, PORX, PERX, PERY, PERZ
          read(1, 102) X1, X2, X3
          TEMP = X2
                                                  if(NEOS == 1)then
!************************ EOS9 ---> EOS3 ****************************
          IF(X1 .LT. 1.0d0) THEN
               SL = X1
            if(yn_sz == 'Y') then
!--------- Set saturated zones to prevent air from being trapped-----
               do j = 1, n_sz
                    if(x(i) > xmin(j) .and. x(i) < xmax(j) .and. &
                         z(i) > zmin(j) .and. z(i) < zmax(j)) then
                         zi = (z(i) - zmin(j)) / (zmax(j) - zmin(j))
                         xc = (xmin(j) + xmax(j)) / 2.0d0
                         SLz = 1.0d0 - zi * (1.0d0 - SL0)
                         if(x(i) < xc) then
                              xi = (x(i) - xmin(j)) / (xmax(j) -xmin(j))
                         else
                              xi = (xmax(j) - x(i)) / (xmax(j) -xmin(j))
                         endif
                         SLx = 2.0d0 * xi * (1.0d0 - SL0) + SL0
                         SL = (SLz + SLx) / 2.0d0
                         if(SL < X1) SL = X1
                         goto 300
```

```
                    endif
                enddo
300         continue
             endif
                X1 = PRES
                SG = 1.0d0 - SL
                X2 = 10.0d0 + SG
            ELSE
                X2 = XX2
!               X1 = PRES *(1.0d0 + 1.0d-6)
!               X1 = X1 + PSAT
            ENDIF
            X3 = TEMP
!-----------------------------------------------------------------------
            write(2, 102) X1, X2, X3
                                                        else
!************************ EOS9 ---> EOS9 ****************************
            if(X1 < 1.0d0 .and. yn_sz == 'Y') then
!--------- Set saturated zones to prevent air from being trapped-----
                do j = 1, n_sz
                    if(x(i) > xmin(j) .and. x(i) < xmax(j) .and. &
                        z(i) > zmin(j) .and. z(i) < zmax(j)) then
                        zi = (z(i) - zmin(j)) / (zmax(j) - zmin(j))
                        xc = (xmin(j) + xmax(j)) / 2.0d0
                        SLz = 1.0d0 - zi * (1.0d0 - SL0)
                        if(x(i) < xc) then
                            xi = (x(i) - xmin(j)) / (xmax(j) -xmin(j))
                        else
                            xi = (xmax(j) - x(i)) / (xmax(j) -xmin(j))
                        endif
                        SLx = 2.0d0 * xi * (1.0d0 - SL0) + SL0
                        SL = (SLz + SLx) / 2.0d0
                        if(SL > X1) X1 = SL
                        goto 301
                    endif
                enddo
301         continue
            endif
!-----------------------------------------------------------------------
            write(2, 102) X1, X2
                                                        endif
      enddo
            read(1, 101) EL, NE, NSEQ, NADD, PORX, PERX, PERY, PERZ
            if(EL=='+++') then
                EL='   '
                write(2, 103) EL
                read(1, 104) atime_step
                write(2,104) atime_step
            endif
100 format(a31, i5, a33)
101 format(a3, a2, 2a5, 4e15.8)
102 format(3E20.13)
103 format(a3)
104 format(a45)
111 format(a5, i5, 7E10.4)
```

```
112 FORMAT(A3, a2, 2a5, A3, A2, 3E10.4, 3F10.4)
121 format(1x/' 1: EOS9 -> EOS3'/' 2: EOS9 -> EOS9'/' Select: [1]')
!999 continue
      close(1)
      close(2)
      end
```

A.2. Calculating water residence time, modified from shareware EXT

```
      program ext
      implicit none
            ……
      integer nxyz
      real(8) vol,dx_1,dy_1,dz_1(60000),t_x, t_z, t_o ! t_x, t_z: water residence time (selected units).
      common/t_res/dx_1,dy_1,dz_1
       integer it_unit
      real(8) t_unit
       write(*,101)
101   format('Please select unit for water residence time:',/
     &  '      1. year',/,'      2. day',/,'      3. second',/,
     &  '      Default: day',/)
      read(*,*) it_unit
       t_unit= 1.0d0/86400.d0
       if(it_unit == 1) t_unit= 1.0d0/(365.25d0*86400.d0)
       if(it_unit == 3) t_unit= 1.0d0
c
c     read arguments
            ……
              open(unit = 3,file=file,status='old')
            else if(file .eq. '-t' .and. i .lt. l) then
              i = i + 1
              call getarg(i, file)
              open(unit = 12, file=file, status='unknown')
            else if(file .eq. '-w' .and. i .lt. l) then
              ……
          write(6,'(a,$)') 'Input file name: '
          read(5,'(a)') file
       print *, 'file=', file
      endif
c
            ……
c     read mesh file
c
      call rmesh(ne,id,x,ec,e,a,cc,hsh,ind,mnel,mncon,nhsh,ixyz)
            ……
      call inspect(cprnt,cprnt,lprnt,l1,k)
      write(6,30) cprnt(lprnt:4),line(3:20)
      write(12,30) cprnt(lprnt:4),line(3:20)
 30   format(' Found printout(',a,'): ',a)
c
c     open output file
            ……
 220  do i = 1, ne1
        j = zo(i)
!         write(2,'(1p,50e14.6)') (x(k,j),k=1,nxyz),(v(k,j),k=1,nv)
```

```
        if(abs(v(nv-1,j)) < 1.0d-56) then
           t_x = 1.0d51
         else
           t_x = dx_1 / abs(v(nv-1,j)) * t_unit
         endif
        if(abs(v(nv,j)) < 1.0d-56) then
           t_z = 1.0d51
         else
           t_z = dz_1(j) / abs(v(nv,j)) * t_unit
         endif
         t_o = t_x * t_z / (t_x + t_z)          ! 09/06/2007.
        write(2,'(1p,50e14.6)') (x(k,j),k=1,nxyz),(v(k,j),k=1,nv)
     &     ,t_x,t_z,t_o
      enddo
            ……
 240  close (unit=1)
       close (unit=12)
      stop
      end

      subroutine rmesh(ne,id,x,ec,e,a,cc,hsh,ind,me,mc,nh,ixyz)
      implicit none
      integer ne,ixyz
            ……
      integer nu2
      real(8) vol,dx_1,dy_1,dz_1(60000)
      common/t_res/dx_1,dy_1,dz_1
      open(unit=1,file='MESH',status='old')
      read(1,'(a)',end=10) wrd
      if(wrd .ne. 'eleme' .and. wrd .ne. 'ELEME') then
        stop 'no eleme in MESH'
      endif
      ne = 0
      locat = 1
! 20   read(1,'(a,45x,3e10.4)',end=10) id(ne + 1),x1,y1,z1
 20   read(1,100,end=10) id(ne + 1),vol,x1,y1,z1
100   format(a,15x,e10.4,20x,3e10.4)
      if(ne==0) then
       ! for 2-d case with constant Y, and the center of the first element is at the origin of coordinates.
          dx_1 = 2.0d0 * x1
          dy_1 = 2.0d0 * y1
       endif
      dz_1(ne+1) = vol/(dx_1 * dy_1)
      x(1,ne+1) = x1
            ……
      return
      end
```

A.3. Calculating distribution coefficient and retardation factor for every grid block at specified times

```
!  Ext_C.f90
!      This program can be used to extracting the input files for Techplot
!      from the output files of TOUGHREACT's concentration, mineral and gas data.
!      A grid file is needed which can be prepared by first running the EXT program
```

```
!     on the output file of flow (flow.out). Just put the 'Zone' line and the J
!     lines of 'MESH' for the structure of the domain.
!     A list of time zones will be write to file 'zone_list.out'.
!     01/12/2006.
!     izone      : zone number
!     nz         : character type, number of zones, used in output file names
!     f_in       : input file name
!     f_out      : output file names
!
! Added code for calculating Kd and Rf. 09/10/2007.
!
            program Ext_C
            implicit none
            character(20) f_in, f_out, cg, f_min
            character(260) line,line1,line_min,var,cgrid,cgrid1(50000)
            character(3) nz
            character(1) kdrf, am  ! KdRf, (Aq or Min)
            character(44) form1, form2
            integer i,j,k,iinf, ng, j_phi, j_w, j_sl, j_c, kt
            integer izone,iline, l, l1, j_max, jm_max,n,imax
            real(8) x(30), y(20000,20),r_rho
!
            print *, 'Input file name: '
            read(*,'(a)') f_in
            open(16, file='zone_list.out', status='unknown')
            write(16, *)' ------ Time Zones ------'
            write(16, *)'   No.         Time Zones'
            print *, 'Calculate Kd and Rf, Yes/No (y/n)?'
            read(*,'(a)') kdrf
            if(kdrf == 'y' .or. kdrf == 'Y') then
              kdrf = 'y'
          print *, 'Input file name for mineral and exchanged species:'
              read(*,'(a)') f_min
              open(21, file=f_min, status='old')
          form1 = '(2F11.3,F10.3,e12.4,2F8.4,F8.3,F8.4,50E12.4)'
          form2 = '(2F11.3,F10.3,F8.3,F10.5,e13.5,60E12.4)'
            else
              print *,'Aqueous or Minerals (A/M)?'
              read(*,'(a)') am
              if(am == 'm' .or. am == 'M') then
            am = 'm'
                  form1 = '(2F11.3,F10.3,F8.3,F10.5,e13.5,60E12.4)'
              else
                am = 'a'
            form1 = '(2F11.3,F10.3,e12.4,2F8.4,F8.3,F8.4,50E12.4)'
              endif
            endif
!
            izone=0
            iline=0
            f_out=f_in
            l = len_trim(f_out)
            k = 0
            r_rho=1.d0/2.65d0 ! reciprocal of rho_s, rho_s = 2.65 Mg/m^3 or kg/L.
            open(15, file='grid', status='old')
```

```
10        continue
          read(15, '(a)', end=20) line
          if(line(1:4) == 'Zone') then
               cgrid = trim(line(5:))
               do n=1,230
                 if(line(n:n+1) == 'I=') then
                   read(line(n+2:n+6),'(i5)')imax
                   goto 43
                 endif
               enddo
43             print *, 'Imax = ', imax
               goto 20
          endif
          goto 10
20        j = len_trim(cgrid)
          cg = '0'
          do i = 1, j-2
               if(cgrid(i:i+1) == 'J=') then
                    cg = cgrid(i+2:j)
               endif
          enddo
          read(cg, '(i)') ng
                    do i = 1, ng
                         read(15, '(a)', end=31) line
                         cgrid1(i) = trim(line)
                    enddo
          close(15)
31     continue
!
! --- For calculating Kd and Rf. 09/10/2007. ---
        if(kdrf == 'y') then
40              read(21, '(a)', end=49) line_min
                if(line_min(1:9)=='VARIABLES') then
                     j = 1
             do i=1, 237
                        if(line_min(i:i+3) == 'Poro') j_phi = j
                        if(line_min(i:i+3) == 'sr+2') j_w = j
                        if(line_min(i:i) == ',') j = j + 1
             enddo
                                jm_max = j - 1
                         print *, 'j_phi, j_w, jm_max = ', j_phi, j_w, jm_max
                         goto 49
                endif
                       goto 40
49           continue
                       endif
! ---------------------------------------------
!
          open(11, file=f_in, status='old')
30        read(11, '(a)', end=90) line
          if(line(1:9)=='VARIABLES') then
            var=trim(line)
!
        if(kdrf == 'y') var = trim(line)//'Kd         ,Rf'
!
```

```
              j = 1
            do i=1, 237
                                if(line(i:i+1) == 'Sl') j_sl = j
                                if(line(i:i+3) == 'sr+2') j_c = j
                                if(line(i:i) == ',') j = j + 1
                        enddo
                        j_max = j - 1
                        print *, 'j_sl, j_c, j_max=', j_sl, j_c, j_max
!             endif
! ------------------------------------------------
!
              goto 30
            elseif(line(1:4)=='ZONE') then
!                       line1=' Time: '//trim(line)
                        line1=trim(line)
                        write(nz,'(i3)') izone
                        write(16, '(i6, 5x, a)') izone, line(6:25)
                        if(nz(1:1) == ' ') nz(1:1)='0'
                        if(nz(2:2) == ' ') nz(2:2)='0'
                        if(nz(3:3) == ' ') nz(3:3)='0'
                        f_out(l+1:l+7) = nz//'.out'
                        print *, 'Output file:  ',f_out
                                open(unit=12,file=f_out,status='unknown')
                        write(12, '(a)') trim(var)
                        write(12, '(a)') trim(line1)
                        write(12, '(a)') trim(cgrid)
                        izone=izone+1
!
          if(kdrf == 'y') then
                          read(21, '(a)') line_min
                          if(line_min(1:4)=='ZONE') then
                            do i=1,imax
                              read(21,form2) (y(i,j), j=1,jm_max)
                            enddo
                          endif
                        endif
! ------------------------------------------------------
          do i=1,imax
                read(11,form1) (X(j),j=1,j_max)
                        if(kdrf =='y') then
                        x(j_max+1) = y(i,j_w)*y(i,j_phi)*x(j_sl)*r_rho/x(j_c) &
                           /(1.d0-y(i,j_phi))
                        x(j_max+2) = 1.d0 + y(i,j_w) / x(j_c)
                           write(12, form1) (x(j), j=1,j_max+2)
                        else
                           write(12, form1) (x(j), j=1,j_max)
                        endif
                      enddo
                                do i = 1, ng
                                        write(12, '(a)') trim(cgrid1(i))
                                enddo
                      close(12)
!                     k = 1
                      goto 30
            else
```

```
                goto 30
          endif
90        close(11)
          close(15)
          close(16)
        if(kdrf =='y') close(21)
          end program Ext_C
```

B. TOUGHREACT CODE MODIFICATIONS FOR MASS BALANCE COMPUTATION

B.1. treact.f

B.1.1. SUBROUTINE COUPLE(next_tstep)

```
            ......
      double precision densw,deltat0
      common/decaym/dec_m(mnel,mpri)
      common/exchange2/SL2
      common/exchange3/xcads_0(mnod,mexc)
      common/cmb/CM_in(MNEL,MPRI),CM_out(MNEL,MPRI),CM_ini(MNEL,MPRI)
C
      SAVE ICALL
            ......
c--------Solve linear equations for aqueous transport (loop 120) ------
c          ------------------------------------------------------
!
! Decay for mass balance output.
        if(icall == 1) then
          do 520 k=1,npri
            do 520 i=1,nel
               dec_m(i,k)=0.0d0
520         continue
        endif
!
c
      DO 120 K=1,NPRI
            ......
       call DRY_MAP
c
       DO 1000 I=1,NNOD
c
c---------- moved sg1 redefinition here, below 499 point
c    Redefine sg1 in case we did not go through matrixg, where sg1 is defined
c    (needed for case when no gas transport occurs (ngas1=0))
         sg1(i) = 1.d0-sl1(i)
c
         phisl1 = phi(i)*sl1(i)
!
         phislo = PHIOLD(i)*SLOLD(i)
!
c
        if (kcpl.EQ.2) then       ! only monitoring porosity change
            ......
c   cation exchange contribution to total concentrations
        do k=1,nexc
          do n=1,npri
!            tt(n)=tt(n)+stqx(k,n)*xcads(i,k)
             tt(n)=tt(n)+stqx(k,n)*xcads(i,k) / phisl1*phislo
!
          end do
        end do
c
500     continue
c
```

```
            ......
C----------------------------------Call geochemical subroutine for each node
       ielem = i
c
!
         SL2 = sl1(i)
!
       CALL NEWTONEQ(ielem,densw)       !ns98/3 added i argument !ns 7/21/01 added densw                    .....
       if(kcpl.eq.1.and.mopr(6).eq.1) call levscale
c
!       CALL  COMPUTE_MASS(icall,deltat0)
       CALL  COMPUTE_MASS(deltat0)
!       NWMAS=10*NWTI
!       IF(MOPR(8).EQ.1 .AND. MOD(KCYC,NWMAS).EQ.0) CALL WRITE_MASS
!
       NWMAS=NWTI
       IF(MOPR(8).EQ.1 .AND. MOD(KCYC,NWMAS).EQ.0)
     1     CALL WRITE_MASS(deltat0)
!
c
      DO 220 I=1,nnod
c
            ......
```

B.1.2. SUBROUTINE MATRIXC_Kdd(IPRI)

```
            ......
      COMMON/BC/NELA
      COMMON/E3/EVOL(MNEL)
      common/decaym/dec_m(mnel,mpri)
       real*8 evoli, phislov, dec_mt(mnel,mpri)
C
c-------------------------------------------------------------------------
C
      SAVE ICALL
        IF (SDEN2.GT.0.0D0 .AND. VKD2.GE.0.0D0)  THEN
          R(N)=R(N) + (1.0D0-PHIOLD(N))*UTOLD(N,IPRI)*SDEN2*VKD2 ! for Kd
          CO(N)=CO(N)+PHI(N)*SL1(N)*Dlamda*DELTEX+
     +          (1.0D0-PHI(N))*SDEN2*VKD2*(1.0d0+Dlamda*DELTEX)
        END IF
!
! Decay for mass balance output.
         if(dlamda > 0.0d0) then
          if(evol(n) >= 1.0d+50 .or. evol(n) <= 0.0d0) then

           else
!     For aqueous species.
            evoli=evol(n)*1000.d0
            phislov = evoli*phiold(n)*slold(n)
             dec_mt(n,ipri) = phislov*utold(n,ipri) * dlamda*deltex
             dec_m(n,ipri) = dec_m(n,ipri) + dec_mt(n,ipri)
!            dec_m(n,ipri)=dec_m(n,ipri)+phislov*utold(n,ipri)
!     +          *(1.0d0-dexp(-dlamda*deltex))

!     For solid species.
            IF (SDEN2.EQ.0.0D0 .AND. VKD2.GE.1.0D0)  THEN
```

```
            RETARD1=VKD2-1.0D0       ! R1=R-1
           END IF
           IF (SDEN2.GT.0.0D0 .AND. VKD2.GE.0.0D0)  THEN
          RETARD1=(1.0D0-PHIOLD(n))*SDEN2*VKD2/(PHIOLD(n)*SLOLD(n))
           END IF
          dec_mt(n,ipri) = dec_mt(n,ipri)+phislov*utold(n,ipri)
    +          *retard1*dlamda*deltex
          dec_m(n,ipri) = dec_m(n,ipri)+phislov*utold(n,ipri)
    +          *retard1*dlamda*deltex
!          dec_m(n,ipri)=dec_m(n,ipri)+phislov*utold(n,ipri)*retard1
!    +           *(1.0d0-dexp(-dlamda*deltex))
!
         endif
        endif
!
C
200     CONTINUE
C
100   CONTINUE
C
     RETURN
     END
c
```

B.1.3. SUBROUTINE VARIABLE_DECAY(N,DLAMDA)

```
C
C---------For Geothermex,minh Pham
C
C**** Calculate decay constant as a function of temperature or (other variables)****
C
     implicit double precision (a-h,o-z)
     implicit integer (i-n)
! Added by L. Wang, 01/18/2006.
       include 'T2'
! End addition.
     COMMON/E6/T(MNEL)
C
     TK=T(N)+273.15D0
     DLAMDA_LN=29.61D0-17236.0D0/TK
     DLAMDA=EXP(DLAMDA_LN)      ! 1/day
     DLAMDA=DLAMDA/86400.0D0     ! 1/s
C
     RETURN
     END
c
```

B.1.4 SUBROUTINE CYCIT

```
            ......
     common/dry_salt/nsalt,isalt(0:mmin)
!
       COMMON/G4/ELEG(MNOGN)
        common/cmb/CM_in(MNEL,MPRI),CM_out(MNEL,MPRI),CM_ini(MNEL,MPRI)
!
C
C-------------------------------------------------------------------------------
```

```
C
c---------- save Henry's constant for air solubility in water
      SAVE HC
            ......
```

B.2. geochem.f

B.2.1. subroutine cx_ct

```
            ......
       double precision dum(mexc),bx(mexc)
!
!
      COMMON/SOLUTE6/SLOLD(MNEL)
      common/exchange2/SL2
!
!
c
       SAVE ICALL
            ......
c       conversion of bx (eq. fraction) into cx (mol solute ads/dm3 sol)
!       cecmol=cec2*2.65d0*(1.d0-phi2)*1.d-2/phi2
!
! According to Dr. Larry Hull, the mass was not balanced for cation exchange using the original codes.
!
       if(SL2 > 0.0d0)
     +    cecmol=cec2*2.65d0*(1.d0-phi2)*1.d-2/(phi2*SL2)
!
       do 400 j=1,nexc
c       gaines&thomas and gapon conventions
            ......
```

B.2.2. subroutine dcx_dcp

```
c
c****************** Evaluate derivatives for cation exchange ******************
c
       implicit double precision (a-h,o-z)
       implicit integer (i-n)
       include 'T2'
       include 'chempar23.inc'
       INCLUDE 'common23.inc'
       double precision cxold(mexc)
!
       COMMON/SOLUTE6/SLOLD(MNEL)
       common/exchange2/SL2
!
c
       SAVE ICALL
            ......
```

B.2.3. ! SUBROUTINE COMPUTE_MASS(icall,deltat0)

```
      SUBROUTINE COMPUTE_MASS(deltat0)
            ......
     integer icall
     double precision deltat0, evoli, phislov
c
!
```

```
       INTEGER NI
      COMMON/WRICON/ NWXY,NWDIM,NWTI,NWNOD,NWCOM,NWMIN,IWNOD(maqx),
     1               IWCOM(maqx),IWMIN(mmin),NWTS,NWTT,IWCOMT
      COMMON/BC/NELA
      COMMON/C1/NEX1(MNCON)
      COMMON/C2/NEX2(MNCON)
      COMMON/C5/AREA(MNCON)
       common/cmb/CM_in(MNEL,MPRI),CM_out(MNEL,MPRI),CM_ini(MNEL,MPRI)
       real*8 cm_now(mnel,mpri)
      SAVE ICALL
      DATA ICALL/0/
      ICALL=ICALL+1
!
      IF(ICALL.EQ.1) WRITE(11,899)
!  899   FORMAT(6X,'COMPUTE_MASS 1.0   30 July     2003',6X,
!
899   FORMAT(6X,'COMPUTE_MASS 1.0   2 February  2007',6X,
     X  'Compute mass input to and output from the system')
!
! ******* Calculating cell mass balance. *****
! ----------------------------------------------For calculating & printing initial mass balance.
!
     IF (ICALL .EQ. 1)  THEN
       OPEN (UNIT=381,FILE='cellmb.out',STATUS='UNKNOWN')
       write(381, 801)
801     format(1x,'Mass (mol) balance for specified cells.',/1x,
     1  'Step_no   Time_step(s)   ELEM   Component      M_in      ',
     2  ' M_out       M_ini       M_cur       M_bal     M_err(%)')
       do I=1,NNOD
        do m=1,nmin
                    pre0(i,m) = pinit(i,m)  ! total moles of mineral per liter medium (V_tot).
        enddo
       enddo
     END IF
! ------------------------------------------------
       DO 101 INO=1,NWNOD
          I = IWNOD(INO)
         IF (EVOL(I)>=1.0D+50 .OR. EVOL(I)<=0.D0)  GO TO 101
         EVOLI=EVOL(I)*1000.D0
         phislov = EVOLI*PHIOLD(I)*SLOLD(I)
         DO 201 J=1,NPRI
              CM_ini(i,j) = phislov * utold(i,j)
           cm_in(i,j) = 0.0d0
           cm_out(i,j) = 0.0d0
           cm_now(i,j) = 0.0d0
201       CONTINUE
C-------------------------Initial amount of component presented in solid phase
         do m=1,nmin
          ncp=ncpm(m)
          do k=1,ncp
            j=icpm(m,k)
              CM_ini(i,j) = CM_ini(i,j) + stqm(m,k)*pre0(i,m)*evoli
          enddo
         enddo
c
```

```
        do m=1,ngas
         ncp=ncpg(m)
         do k=1,ncp
           j=icpg(m,k)
             CM_ini(i,j) = CM_ini(i,j) + stqg(m,k)*gp(i,m)*evoli
        enddo
        enddo
!
!************************************************** Addition for Kd adsorption
!
    IF (NKDD .GT. 0)    THEN
      DO J=1,NPRI
!
!--solid density (kg/dm**3), and Kd(l/kg=mass/kg solid / mass/l water)
!
         KDDS=KDDP(J)       ! Number in the species list for Kd and decay
         IF (KDDS .EQ. 0)  GO TO 402
         KDDZONE=IZONEKD(I)    ! Kd zone code
         IF (KDDZONE .LE. 0)  THEN
           SDEN2=0.0D0
           VKD2=1.0D0
           GO TO 401
         END IF
         SDEN2=SDEN(KDDZONE,KDDS)  ! solid density
         VKD2=VKD(KDDZONE,KDDS)    ! Kd value; or r factor if solid density=0
401        CONTINUE
!
         IF (SDEN2.EQ.0.0D0 .AND. VKD2.GE.1.0D0)  THEN
!----------------If density is zero vkd2 is retardation factor
           RETARD1=VKD2-1.0D0       ! R1=R-1
         END IF
         IF (SDEN2.GT.0.0D0 .AND. VKD2.GE.0.0D0)  THEN
           RETARD1=(1.0D0-PHIOLD(I))*SDEN2*VKD2/(PHIOLD(I)*SLOLD(I))
         END IF
            CM_ini(i,j) = CM_ini(i,j) + phislov*UTOLD(I,J)*RETARD1
!
402        CONTINUE
       END DO
    END IF
!
!*********************************************************************
!
        do m=1,nads
         ncp=ncpad(m)
         do k=1,ncp
           j=icpad(m,k)
             CM_ini(i,j) = CM_ini(i,j) + stqd(m,k)*d(i,m)*phislov
         enddo
        enddo
!
!********************************************** Addition for exchange
!
        do k=1,nexc
          do j=1,npri
              CM_ini(i,j) = CM_ini(i,j) + stqx(k,j)*xcads(i,k)*phislov
```

```
            end do
          end do
!
!**********************************************************************
!
101     continue
! End addition.
!
c
C---------------------------------------Set variables to zero at the beginning
             ......
C-------------------------------Calculate mass entering and leaving the system
      DO 140 IOGN=1,NOGN
        J=NEXG(IOGN)
c
c*****************************************************
        NLOC2=(J-1)*NSEC*NEQ1
        IF (IEOS .NE. 9)         THEN     ! for other modules
          NLOC2L=NLOC2+NBK
          densw = PAR(NLOC2L+4)
                           ELSE     ! for eos9 module
          densw=PAR(NLOC2+4)
        END IF
C*****************************************************
c
        vliqw = densw/1.d3
        IF(LCOM(IOGN).EQ.1 .AND. G(IOGN).GE.0.D0) THEN
          IZONEJ=IZONEBW(J)
          DO 160 IPRI=1,NPRI
!             SOLUTINP(IPRI)= SOLUTINP(IPRI) + G(IOGN)
!    +                  *UB(IZONEJ,IPRI)*deltat0/vliqw
!
! Since UB is in mols per kg water. See Line 1042 of inichm.f.
!
            SOLUTINP(IPRI)= SOLUTINP(IPRI) + G(IOGN)
     +                  *UB(IZONEJ,IPRI)*deltat0
!
160       CONTINUE
        END IF
        IF(LCOM(IOGN).EQ.1 .AND. G(IOGN).LT.0.D0) THEN
          DO 180 IPRI=1,NPRI
            SOLUTOUT(IPRI)= SOLUTOUT(IPRI) - G(IOGN)*UT(J,IPRI)
     +                  *deltat0
180       CONTINUE
        END IF
140   CONTINUE
C
!
!
! Calculate mass leaving the system through bottom Dirichlet boundary.
!
       DO 303 N=1, NCON
          N1=NEX1(N)
          N2=NEX2(N)
          NI=(N-1)*NPH+NPL
```

```
          IF(N1 == 0 .OR. N2 == 0) GOTO 303
         IF(N1 > NELA .AND. N2 > NELA) GOTO 303
         IF(EVOL(N2) >= 1.0D+50 .OR. EVOL(N2) <= 0.0D0) THEN
           IF(VELDAR(NI) < 0.0D0) THEN
                      DO 310 IPRI=1,NPRI
              SOLUTOUT(IPRI)= SOLUTOUT(IPRI) - VELDAR(NI)
   +            *AREA(N)*1.D3*UTold(N1,IPRI)*deltat0

310            CONTINUE
           ELSE    ! RECHARGE BY THE BOUNDARY.

              ENDIF
! In case the boundary grid block is set in N1. 11/23/2006.
         ELSEIF(EVOL(N1) >= 1.0D+50 .OR. EVOL(N1) <= 0.0D0) THEN
           IF(VELDAR(NI) > 0.0d0) THEN
                      DO 320 IPRI=1,NPRI
              SOLUTOUT(IPRI)= SOLUTOUT(IPRI) + VELDAR(NI)
   +            *AREA(N)*1.D3*UTold(N2,IPRI)*deltat0
320            CONTINUE
           ELSE    ! RECHARGE BY THE BOUNDARY.

              ENDIF
         ENDIF
303     CONTINUE
!
!
C--------------Calculate mass entering and leaving the system by gas diffusion
C
     IF (NGAS1.LE.0)   GO TO 299
     IF (NGAS1.GT.0)  Then
       DO 240 I=1,NELG
        DO M=1,NGAS
          ncp=ncpg(m)
          do k=1,ncp
           j=icpg(m,k)
           IF (QG(I,M).GE.0.0D0)     THEN
             SOLUTINP(J)= SOLUTINP(J) +
   +                 QG(I,M)*stqg(m,k)
!                              ELSE
! In case QG(I,M) == .null.
             ELSEIF(QG(I,M) .LT. 0.0D0) THEN
!
             SOLUTOUT(J)= SOLUTOUT(J) -
   +                 QG(I,M)*stqg(m,k)
           END IF
         enddo
       enddo
240     CONTINUE
      Endif
299   CONTINUE
C
!
! ****** Cell mass balance. ******
! ***************************************************************
!
```

```
      DO 141 IOGN=1,NOGN
        J=NEXG(IOGN)
        IF(LCOM(IOGN).EQ.1 .AND. G(IOGN).GE.0.D0) THEN
          IZONEJ=IZONEBW(J)
          DO 161 IPRI=1,NPRI
            cm_in(j,ipri) = cm_in(j,ipri) + G(IOGN)
     +                  *UB(IZONEJ,IPRI)*deltat0
  161       CONTINUE
        END IF
        IF(LCOM(IOGN).EQ.1 .AND. G(IOGN).LT.0.D0) THEN
          DO 181 IPRI=1,NPRI
            cm_out(j,ipri) = cm_out(j,ipri) - G(IOGN)
     +                  *UB(J,IPRI)*deltat0
  181       CONTINUE
        END IF
  141   CONTINUE
!
! Calculate mass entering or leaving the cell through advection.
        DO 306 N=1, NCON
          N1=NEX1(N)
          N2=NEX2(N)
          NI=(N-1)*NPH+NPL
            IF(N1 == 0 .OR. N2 == 0) GOTO 306
          IF(N1 > NELA .AND. N2 > NELA) GOTO 306
          IF(EVOL(N2) < 1.0D+50 .and. EVOL(N2) > 0.0D0) THEN
            IF(VELDAR(N) < 0.0D0) THEN
                        DO 411 IPRI=1,NPRI
              cm_in(N2,IPRI) = cm_in(N2,IPRI) - VELDAR(NI)
     +             *AREA(N)*1.D3*UTold(N1,IPRI)*deltat0
  411             CONTINUE
            ELSE
                        DO 412 IPRI=1,NPRI
              cm_out(N2,IPRI) = cm_out(N2,IPRI) + VELDAR(NI)
     +             *AREA(N)*1.D3*UTold(N2,IPRI)*deltat0
  412             CONTINUE
              ENDIF
          ENDIF
! In case the boundary grid block is set in N1. 11/23/2006.
          IF(EVOL(N1) < 1.0D+50 .and. EVOL(N1) > 0.0D0) THEN
            IF(VELDAR(N) < 0.0D0) THEN
                        DO 415 IPRI=1,NPRI
              cm_out(N1,IPRI) = cm_out(N1,IPRI) - VELDAR(NI)
     +             *AREA(N)*1.D3*UTold(N1,IPRI)*deltat0
  415             CONTINUE
            ELSE
                        DO 414 IPRI=1,NPRI
              cm_in(N1,IPRI) = cm_in(N1,IPRI) + VELDAR(NI)
     +             *AREA(N)*1.D3*UTold(N2,IPRI)*deltat0
  414             CONTINUE
              ENDIF
          ENDIF
  306   CONTINUE
!
C--------------Calculate mass entering and leaving the cell by gas diffusion
C
```

```
      if (NGAS1.GT.0) then
       DO I=1,NELG
        ia = ielg(i)
       DO M=1,NGAS
         ncp=ncpg(m)
         do k=1,ncp
          j=icpg(m,k)
          IF (QG(I,M).GE.0.0D0)     THEN
            cm_in(ia,j)= cm_in(ia,j) +
   +                 QG(I,M)*stqg(m,k)
            ELSEIF(QG(I,M) .LT. 0.0D0) THEN
            cm_out(ia,j)= cm_out(ia,j) -
   +                 QG(I,M)*stqg(m,k)
          END IF
         enddo
       enddo
       enddo
      endif
!
!
      RETURN
      END
```

B.2.4. ! SUBROUTINE WRITE_MASS

```
      SUBROUTINE WRITE_MASS(deltat0)
           ......

      common/Kddca7/nkdd          ! number of species with Kd adsorption
!
      common/decaym/dec_m(mnel,mpri)
      double precision mbout(mpri)
      COMMON/CYC/KCYC,ITER,ITERC,TIMIN,SUMTIM,GF,TIMOUT
       common/cmb/CM_in(MNEL,MPRI),CM_out(MNEL,MPRI),CM_ini(MNEL,MPRI)
       real*8 CM_now(mnel,mpri),CM_bal,CM_err,dec_mt(mnel,mpri)
!
C-------------------------------------------------------------------------
c
      SAVE ICALL
      DATA ICALL/0/
      ICALL=ICALL+1
      IF(ICALL.EQ.1) WRITE(11,899)
!  899   FORMAT(6X,'WRITE_MASS   1.0   30 July     2003',6X,
!
  899   FORMAT(6X,'WRITE_MASS   1.0   2 February  2007',6X,
           ......
      DO 400 I=1,NNOD
!
!        IF (EVOL(I).GE.1.0D+10)  GO TO 400
!
        IF (EVOL(I).GE.1.0D+50 .OR. EVOL(I).LE.0.0D0)  GO TO 400
!
!
        EVOLI=EVOL(I)*1000.D0
          ......
400     continue
```

```
!
! Mass balance for specified cells.
!
!----------------- Current amount of component presented in aqueous phase
      DO 401 INO=1,NWNOD
         I = IWNOD(INO)
        IF (EVOL(I).GE.1.0D+50 .OR. EVOL(I).LE.0.0D0)  GO TO 401
        EVOLI=EVOL(I)*1000.D0
        phislv = evoli*phiold(i)*sl1(i)
        DO 501 J=1,NPRI
           cm_now(i,j) = phislv*UT(i,j)
501       CONTINUE
!
!----------------- Current amount of component presented in solid & gas phase
       do m=1,nmin
         ncp=ncpm(m)
         do k=1,ncp
           j=icpm(m,k)
            cm_now(i,j) = cm_now(i,j) + stqm(m,k)*pre(i,m)*evoli
         end do
       end do
!
       do m=1,ngas
         ncp=ncpg(m)
         do k=1,ncp
           j=icpg(m,k)
            cm_now(i,j) = cm_now(i,j)+stqg(m,k)*gp(i,m)*evoli
         enddo
       enddo
!
!------------------- Addition for Kd adsorption
!
    IF (NKDD .GT. 0)    THEN
      DO J=1,NPRI
!
!--solid density (kg/dm**3), and Kd(l/kg=mass/kg solid / mass/l water)
!
         KDDS=KDDP(J)       ! Number in the species list for Kd and decay
         IF (KDDS .EQ. 0)  GO TO 402
         KDDZONE=IZONEKD(I)    ! Kd zone code
         IF (KDDZONE .LE. 0)  THEN
           SDEN2=0.0D0
           VKD2=1.0D0
           GO TO 403
         END IF
         SDEN2=SDEN(KDDZONE,KDDS)  ! solid density
         VKD2=VKD(KDDZONE,KDDS)    ! Kd value; or r factor if solid density=0
403       CONTINUE
!
         IF (SDEN2.EQ.0.0D0 .AND. VKD2.GE.1.0D0)  THEN
!---------------- If density is zero vkd2 is retardation factor
           RETARD1=VKD2-1.0D0       ! R1=R-1
         END IF
         IF (SDEN2.GT.0.0D0 .AND. VKD2.GE.0.0D0)  THEN
           RETARD1=(1.0D0-PHI(I))*SDEN2*VKD2/(PHI(I)*SL1(I))
```

```
          END IF
            cm_now(i,j) = cm_now(i,j)+phislv*UT(I,J)*RETARD1
!
402         CONTINUE
        END DO
      END IF
!
!**********************************************************************
!
         do m=1,nads
           ncp=ncpad(m)
           do k=1,ncp
             j=icpad(m,k)
               cm_now(i,j) = cm_now(i,j)+stqd(m,k)*d(i,m)* phislv
           enddo
         enddo
!
!************************ Addition for exchange ************************
!
         do k=1,nexc
            do j=1,npri
              cm_now(i,j) = cm_now(i,j)+stqx(k,j)*xcads(i,k)*phislv
            end do
         end do
!
!**********************************************************************
!
!---------------------Add the amount in residual solids at dry grid blocks
        do j=1,npri
          cm_now(i,j) = cm_now(i,j) + evoli*adryr(i,j)
        end do
!
!----------------------------------------------------------------------
!
401     continue
! For species decay, add to the cm_out for mass balance output.
        do 404 k=1,npri
          do 404 i=1,nnod
           cm_out(i,k) = cm_out(i,k) + dec_mt(i,k)
404     continue

!
!
C
C----------Total of each component in in residual solids at dry blocks
C
        do j = 1,npri
          tdryc(j) = 0.0d0
          do i = 1,nnod
            tdryc(j) = tdryc(j) + EVOL(I)*1000.D0*adryr(i,j)
          end do
        end do
C
C
!
```

```
! For species decay, add to the solutout for mass balance output.
      do 520 k=1,npri
         Mbout(k) = solutout(k)
       do 520 i=1,nnod
         Mbout(k) = Mbout(k) + dec_m(i,k)
520    continue
!
      TIMEDAY=TIMETOT/86400.0D0
      WRITE(37,680) TIMEDAY
680    FORMAT(//1X,'Mass (mol) balance for the whole system at time',
   +         E12.5,' days:'/)
      WRITE(37,685)
685    FORMAT(1X,'-----------------------------------------',
   1   '-----------------------------------------',35('-'))
      WRITE(37,700)
700    FORMAT(1X,' Component       Input         Output              ',
   2   '  Initial                  Current            Residual'
   3    /47X,'Aqueous      Solid+gas       Aqueous       Solid+gas'
   4       /1X,'-----------------------------------------',
   5   '-----------------------------------------',35('-'))
      DO 740 J=1,NPRI
        IF (J.EQ.NW.OR.J.EQ.NH.OR.J.EQ.NE.OR.J.EQ.ND) GO TO 740
!         WRITE(37,760)  NAPRI(J),SOLUTINP(J),SOLUTOUT(J),
!    1                    SOLUTINI(J),SOLIDINI(J),
!    2                    SOLUTNOW(J),SOLIDNOW(J),tdryc(j)
! Above 3 lines were modified in order to see the changes.
         WRITE(37,761)  NAPRI(J),SOLUTINP(J),Mbout(j),    !SOLUTOUT(J),
   1                    SOLUTINI(J),SOLIDINI(J),
   2                    SOLUTNOW(J),SOLIDNOW(J),tdryc(j)
761       FORMAT(2X,A10,7E15.8)
!
760       FORMAT(2X,A10,7E10.3)
740    CONTINUE
      WRITE(32,685)
C-----------------------------------------Calculate mass balance
C
      DO 785 J=1,NPRI
!         balanc1t = balance1(j) !
!         balanc2t = balance2(j) !
         BALANCE1(J)=SOLUTINP(J) +
   1             SOLUTINI(J) + SOLIDINI(J)
c
!         BALANCE2(J)= SOLUTOUT(J) + !
         BALANCE2(J)= mbout(j) +
   1             SOLUTNOW(J) + SOLIDNOW(J)
         BDIFF(J) = BALANCE2(J) - BALANCE1(J)
         RELD(J)=(BDIFF(J)*100.d0)/BALANCE1(J)
         relinp(j) = (SOLIDNOW(J)-SOLIDINI(J))/
   +      (SOLUTINP(J) - (SOLUTNOW(J)- SOLUTINI(J)))
         relinp(j) = (relinp(j)-1.d0)*1.d2
785    CONTINUE
C
      WRITE(37,800)
800    FORMAT(14X,'  Input+Initial      Output+Current       ',
   1  'Difference        Rel. Dif.(%)      Del Solid/liq %') !
```

```
      WRITE(37,685)
      DO 840 J=1,NPRI
        IF (J.EQ.NW.OR.J.EQ.NH.OR.J.EQ.NE.OR.J.EQ.ND) GO TO 840
!         WRITE(37,860)  NAPRI(J),BALANCE1(J),BALANCE2(J),
!    1                   BDIFF(J),RELD(J),relinp(j)
! Above 2 lines were modified in order to see the changes.
         WRITE(37,861)  NAPRI(J),BALANCE1(J),BALANCE2(J),
   1                   BDIFF(J),RELD(J),relinp(j)
861       FORMAT(2X,A10,3X,E16.8,4(4x,E16.8))   !
!
860       FORMAT(1X,A10,2X,E16.8,4X,E16.8,3E16.8)
840     CONTINUE
!
       do ino = 1, nwnod
        i = iwnod(ino)
        if(evol(i) > 0.0d0 .and. evol(i) < 1.0d50) then
         do j = 1,npri
         IF (J.EQ.NW.OR.J.EQ.NH.OR.J.EQ.NE.OR.J.EQ.ND) then

          else
           cm_bal = cm_now(i,j)+cm_out(i,j)-cm_ini(i,j)-cm_in(i,j)
           cm_err = cm_bal / (cm_ini(i,j)+cm_in(i,j)) * 1.0D2
           write(381,802)kcyc,deltat0,elem(i),napri(j),cm_in(i,j),
   1          cm_out(i,j),cm_ini(i,j),cm_now(i,j),cm_bal,cm_err
          endif
         end do
        endif
       end do
      write(381,*)"
802     format(1x,i6,5x,e10.4,3x,a5,3x,a10,6(2x,e10.4))
!
      WRITE(37,685)
C
      RETURN
      END
```

B.3. inichm.f

B.3.1. subroutine init

```
          ......
      character*100 label
!
       real*8 densw
      COMMON/SOLUTE8/SL1(0:MNEL)
      common/exchange2/SL2
!
c
      SAVE ICALL
           ......
       do i=1,naqx
         gamt(i+npri)=gams(i)
       end do
C-----------------------------------------------
c
!
```

```
          SL2 = sl1(N)
!
         call cx_ct
         do j=1,nexc
           xcads(n,j)=cx(j)
         end do
       end if
795   continue
c
              ......
```

B.4. newton.f

B.4.1. subroutine chemeq(it,no_ch,ielem)

```
       common/ion_str2/str_node(mnel)    !ionic strength for all nodes
c----------------------
!
       COMMON/SOLUTE6/SLOLD(MNEL)
       common/exchange2/SL2
       common/exchange3/xcads_0(mnod,mexc)
!
       NGAMM=1
            ......
```

C. SAMPLE PAGES FOR MODEL INPUTS

C.1. flow.inp

```
2D strontium-90 reactive transport
Modified from Yang (2005).
*******************************************************************************
ROCKS----1----*----2----*----3----*----4----*----5----*----6----*----7----*----8
SALLU    2  2650.e00     0.32   9.17e-12  9.17e-12  9.17e-12      2.00     1000.

   7        0.338    0.02100       1.
   7        0.338    0.02000  1.149e-3      1.e7        1.
SAND1    2  2650.e00     0.47   2.18e-13  2.18e-13  2.18e-13      2.00     1000.

   7       0.227       .0210        1.
   7       0.227       .0200  7.717e-5      1.e7        1.
SAND2    2  2650.e00     0.47   2.18e-13  2.18e-13  2.18e-13      2.00     1000.

   7       0.227       .0210        1.
   7       0.227       .0200  7.717e-5      1.e7        1.
BASLS    2  2650.e00     0.05  3.00e-14  3.00e-14  3.00e-13      2.00     1000.

   7        0.6000    0.0011        1.
   7        0.6000    0.0010  1.019e-3      1.e7        1.
BASLT    2  2650.e00     0.05  3.00e-14  3.00e-14  3.00e-13      2.00     1000.

   7        0.6000    0.0011        1.
   7        0.6000    0.0010  1.019e-3      1.e7        1.
BOUND    2  2650.e00     0.05  3.00e-13  3.00e-13  3.00e-13      2.00     1000.

   5        0.6000    0.0011        1.
   8        0.6000    0.0010  1.019e-3      1.e7        1.
REFCO     1.0130e+05     25.00                          -137.464      2.0

MULTI----1----+----2----+----3----+----4
   2    2    2    6
START----1----*----2----*----3----*----4----*----5----*----6----*----7----*----8
----*----1-MOP: 123456789*123456789*1234----*----5----*----6----*----7----*----8
REACT----1MOPR(20)-2----*----3----*----4----*----5----*----6----*----7----*----8
00020001
PARAM----1----*----2----*----3----*----4----*----5----*----6----*----7----*----8
  09999    5000000000000122020371005      2.14e-5     2.334       0.0
      0.06.31152E09 1.000e+011.57788E08              9.8100       4.0
1.000e-005

TIMES----1----*----2----*----3----*----4----*----5----*----6----*----7----*----8
  16  60 1.57788E081.57788E08
3.1549E+073.1558E+073.3286E+073.5878E+073.5886E+076.3115E+077.8894E+079.4673E+07
1.2623E+081.5779E+082.2090E+083.1558E+084.7336E+086.3115E+087.8894E+089.4673E+08
```

C.2. solute.inp

```
'INTEC Sr-90 Transport'
options for reactive chemical transport
   2    1    5  0.3    1    0    0    0    0 ! ISPIA,INIBOUND,ISOLVC,rcour,NGAS1,ichdump,kcpl,Ico2h2o,numdr
constraints for reactive chemical transport  (4e10.4)
  1.00e-6     0.000       8.0       1.0      !sl1min, d1min, stimax
Read input and output file names:
INTEC_thermo.dat                ! thermodynamic database
iter.out                        ! iteration information
INTEC_conc.out                  ! aqueous concentrations in tecplot form
INTEC_min.out                   ! mineral data  in tecplot form
INTEC_gas.out                   ! gas data  in tecplot form
c_vs_time.out                   ! concentrations at specific elements over time
Weighting parameters
      1.0       1.0   2.0d-09     -1.00   ! itime wupc,dffun,dffung
data to convergence criteria:
  50 1.000E-04  300 1.000E-04   50 1.000E-04  1.00E-04  1.00E-04    ! ..... TOLDC,TOLDR
writing control variables:
 100   12   13    2    0    1    2   ! NWTI,NWNOD,NWCOM,NWMIN,IWCOMT,conflag(=1:mol/l),minflag(=1:Vf)
pointer of nodes for writing in time:
JN114ND130JI131KD132KH132JF133KE136IU137J4137KF137LY137P3137
pointer of components for writing:
   2    3    4    5    6    7    8    9   10   11   14   15   16
pointer of minerals for writing:
   1    2
default values of chemical zone codes for grid blocks:
   1    0    1    0    0    1    0    0
chemical zone codes for nodes:
A1199    0    0    1    1    1    1    0    1    0    0
A2199    0    0    1    0    1    1    0    1    0    0
A3199    0    0    1    0    1    1    0    1    0    0
A4199    0    0    1    0    1    1    0    1    0    0
A5199    0    0    1    0    1    1    0    1    0    0
A6199    0    0    1    0    1    1    0    1    0    0
A7199    0    0    1    0    1    1    0    1    0    0
A8199    0    0    1    0    1    1    0    1    0    0
A9199    0    0    1    0    1    1    0    1    0    0
AA199    0    0    1    0    1    1    0    1    0    0
AB199    0    0    1    0    1    1    0    1    0    0
AC199    0    0    1    0    1    1    0    1    0    0
AD199    0    0    1    0    1    1    0    1    0    0
AE199    0    0    1    0    1    1    0    1    0    0
AF199    0    0    1    0    1    1    0    1    0    0
AG199    0    0    1    0    1    1    0    1    0    0
AH199    0    0    1    0    1    1    0    1    0    0
AI199    0    0    1    0    1    1    0    1    0    0
AK199    0    0    1    0    1    1    0    1    0    0
AL199    0    0    1    0    1    1    0    1    0    0
AN199    0    0    1    0    1    1    0    1    0    0
AO199    0    0    1    0    1    1    0    1    0    0
AP199    0    0    1    0    1    1    0    1    0    0
AQ199    0    0    1    0    1    1    0    1    0    0
```

C.3. chemical.inp

```
'INTEC Sr-90 Transport'
'--------------------------------------------------------------------------'
'DEFINITION OF THE GEOCHEMICAL SYSTEM'
'PRIMARY AQUEOUS SPECIES'
'h2o'
'h+'
'ca+2'
'na+'
'al+3'
'cs+'
'sr+2'
'hco3-'
'no3-'
'cl-'
'br-'
'*'
'MINERALS'
'calcite'     0 0 0 0   ! calcite equilibrium phase
  0.0  0.0  0.0        ! precipitates at Q/K = 0  (SAMPLE EOS3: 0.732474 25.0 100.0)
'gibbsite'     0 0 0 0  ! gibbsite equilibrium phase
  0.0  0.0  0.0        ! precipitates at Q/K = 0
'*'          0 0 0 0
'GASES'
'co2(g)'
'*'
'SURFACE COMPLEXES'
'*'
'species with Kd and decay    decay constant(1/s)'
'*'                          0.0d0
'EXCHANGEABLE CATIONS'
'               master     convention     ex. coef.'
'na+'             1           1           1.0
'ca+2'            0           1           0.40
'al+3'            0           1           0.60
'cs+'             0           1           0.08
'sr+2'            0           1           0.35
'h+'              0           1           7.7e+05
'*'               0           0           0.0
'--------------------------------------------------------------------------'
'INITIAL AND BOUNDARY WATER TYPES'
1   2          !niwtype, nbwtype = number of initial and boundary waters
1     25.0     0                       ! pore water chemistry
'       icon        guess         ctot          constrain pore water chemistry'
'h2o'      1        1.000d+00     1.0000d+00        ' '      0
'h+'       3        5.012d-08     5.3690d-08        ' '      0
'ca+2'     1        1.586d-03     1.6400d-03        ' '      0
'na+'      1        3.300d-04     3.3000d-04        ' '      0
'al+3'     1        2.000d-08     2.0000d-08        ' '      0
'cs+'      1        1.000d-17     5.0000d-16        ' '      0
'sr+2'     1        1.000d-17     5.0000d-16        ' '      0
'hco3-'    1        3.240d-03     3.6400d-03        ' '      0
```

C.4. Thermodynamic database

THERMOK with alo2- switched with al+3

******* thermok 2.07 **********

!end-of-header Do not remove this record!
'Temperature points: ' 6 0.0 25.0 60.0 100.0 150.0 200.0
'h2o' 0.00 0.0 18.015
'al+3' 3.33 3.00 26.98 !switched
'ca+2' 2.87 2.0 40.078
'cl-' 1.81 -1.0 35.453
'h+' 3.08 1.0 1.008
'hco3-' 2.10 -1.0 61.017
'k+' 2.27 1.0 39.098
'mg+2' 2.54 2.0 24.305
'na+' 1.91 1.0 22.990
'sio2(aq)' 100.08 0.0 60.084
'so4-2' 3.15 -2.0 96.064
'f-' 1.33 -1.0 18.998
'hfeo2' 0.00 0.0 88.854
'no3-' 2.81 -1.0 62.005
'sr+2' 3.00 2.0 89.908 ! radioactive strontium 90
'cs+' 2.61 1.0 133.907 ! radioactive cesium 134
'cx+' 2.61 1.0 136.907 ! radioactive cesium 137
'br-' 1.96 -1.0 79.904
'null' 0. 0. 0.
'cano3+' 102.083 2.31 1.00 2 1.0000 'ca+2' 1.0000 'no3-'
'cano3+' 500.0000 -0.7000 500.0000 500.0000 500.0000 500.0000
'cano3+' 0.00000000E+00 -0.70000000E+00 0.00000000E+00 0.00000000E+00
0.00000000E+00
'hno3(aq)' 63.013 0.00 0.00 2 1.0000 'h+' 1.0000 'no3-'
'hno3(aq)' 1.5366 1.3025 0.9479 0.5427 0.0413 -0.4704
'hno3(aq)' 0.13221635E+03 -0.84248108E+03 -0.12949984E+00 0.48175787E+05
-0.28888766E+07
'srco3(aq)' 147.629 0.00 0.00 3 -1.0000 'h+' 1.0000 'hco3-' 1.0000 'sr+2'
'srco3(aq)' 8.0055 7.4635 6.8655 6.3400 5.8193 5.3621
'srco3(aq)' 0.14684870E+03 -0.92785686E+03 -0.14239298E+00 0.51261561E+05
-0.27410421E+07
'srno3+' 149.625 2.31 1.00 2 1.0000 'no3-' 1.0000 'sr+2'
'srno3+' 500.0000 -0.8000 500.0000 500.0000 500.0000 500.0000
'srno3+' 0.00000000E+00 -0.80000000E+00 0.00000000E+00 0.00000000E+00
0.00000000E+00
'sroh+' 104.627 2.31 1.00 3 -1.0000 'h+' 1.0000 'h2o' 1.0000 'sr+2'
'sroh+' 500.0000 13.2900 500.0000 500.0000 500.0000 500.0000
'sroh+' 0.00000000E+00 0.13290000E+02 0.00000000E+00 0.00000000E+00
0.00000000E+00
'co2(aq)' 44.01 100.23 0.00 3 -1.0000 'h2o' 1.0000 'h+' 1.0000 'hco3-'
'co2(aq)' -6.5800 -6.3450 -6.2680 -6.3880 -6.7240 -7.1970
'co2(aq)' 0.58981813E+02 -0.37804866E+03 -0.67453194E-01 0.22173326E+05
-0.16542761E+07
'co3-2' 60.0090 2.81 -2.00 2 -1.0000 'h+' 1.0000 'hco3-'
'co3-2' 10.6240 10.3290 10.1300 10.0840 10.2000 10.4650

D. SAMPLE PAGES FOR MODEL OUTPUTS

D.1. flow.out

2D strontium-90 reactive transport

OUTPUT DATA AFTER (****, 2)-2-TIME STEPS   THE TIME IS
0.73050E+05 DAYS

@@@

TOTAL TIME   KCYC   ITER ITERC   KON   DX1M   DX2M   DX3M   MAX. RES.   NER
KER   DELTEX
0.63115E+10 67951   2 135962   2   0.73007E-11 0.10144E-14 0.00000E+00   0.11515E-10   2916   2
0.67610E+05

@@@

ELEM. INDEX   P   T   SG   SL   XAIRG   XAIRL   PER.MOD.   PCAP   DG
DL
(PA)   (DEG-C)   (PA)   (KG/M**3)   (KG/M**3)

A1199   1 0.10105E+06 0.25000E+02 0.68067E+00 0.31933E+00 0.98025E+00 0.15734E-04 0.10000E+01
-.87046E+04 0.11665E+01 0.99716E+03
A2199   2 0.10106E+06 0.25000E+02 0.68067E+00 0.31933E+00 0.98025E+00 0.15735E-04 0.10000E+01
-.87046E+04 0.11666E+01 0.99716E+03
A3199   3 0.10107E+06 0.25000E+02 0.68067E+00 0.31933E+00 0.98025E+00 0.15737E-04 0.10000E+01
-.87046E+04 0.11667E+01 0.99716E+03
A4199   4 0.10107E+06 0.25000E+02 0.68067E+00 0.31933E+00 0.98025E+00 0.15738E-04 0.10000E+01
-.87046E+04 0.11668E+01 0.99716E+03
A5199   5 0.10108E+06 0.25000E+02 0.68067E+00 0.31933E+00 0.98026E+00 0.15740E-04 0.10000E+01
-.87046E+04 0.11669E+01 0.99716E+03
A6199   6 0.10109E+06 0.25000E+02 0.68067E+00 0.31933E+00 0.98026E+00 0.15741E-04 0.10000E+01
-.87046E+04 0.11670E+01 0.99716E+03
A7199   7 0.10110E+06 0.25000E+02 0.68067E+00 0.31933E+00 0.98026E+00 0.15743E-04 0.10000E+01
-.87046E+04 0.11671E+01 0.99716E+03
A8199   8 0.10111E+06 0.25000E+02 0.68067E+00 0.31933E+00 0.98026E+00 0.15744E-04 0.10000E+01
-.87046E+04 0.11672E+01 0.99716E+03
A9199   9 0.10112E+06 0.25000E+02 0.68067E+00 0.31933E+00 0.98026E+00 0.15745E-04 0.10000E+01
-.87046E+04 0.11673E+01 0.99716E+03
AA199   10 0.10112E+06 0.25000E+02 0.68067E+00 0.31933E+00 0.98026E+00 0.15746E-04 0.10000E+01
-.87046E+04 0.11674E+01 0.99716E+03
AB199   11 0.10112E+06 0.25000E+02 0.68067E+00 0.31933E+00 0.98026E+00 0.15746E-04 0.10000E+01
-.87046E+04 0.11674E+01 0.99716E+03
AC199   12 0.10113E+06 0.25000E+02 0.68067E+00 0.31933E+00 0.98026E+00 0.15747E-04 0.10000E+01
-.87046E+04 0.11675E+01 0.99716E+03
AD199   13 0.10114E+06 0.25000E+02 0.68067E+00 0.31933E+00 0.98027E+00 0.15749E-04 0.10000E+01

D.2. mbalance.out

Mass (mol) balance for the whole system at time 0.11840E+00 days:

Component	Input	Output	Initial		Current	Residual
			Aqueous	Solid+gas	Aqueous	Solid+gas
ca+2	0.37917311E+01	0.37925126E+01	0.50404112E+06	0.65826856E+10	0.49640080E+06	0.65826927E+10
na+	0.76297028E+00	0.84603649E+00	0.10142291E+06	0.10079846E+07	0.13051437E+06	0.97888644E+06
al+3	0.46240596E-04	0.42035047E-04	0.61468393E+01	0.88789592E-02	0.56437715E+01	0.51193896E+00
cs+	0.11560156E-11	0.98746409E-12	0.15367107E-06	0.10925056E-04	0.12187674E-06	0.10956785E-04
sr+2	0.11560156E-11	0.94266317E-12	0.15367107E-06	0.32941940E-04	0.11949387E-06	0.32975921E-04
hco3-	0.12654545E+05	0.84571172E+01	0.11187254E+07	0.64805812E+10	0.11268480E+07	0.64805731E+10
no3-	0.23120312E-05	0.23120532E-05	0.30734215E+00	0.00000000E+00	0.30734032E+00	0.00000000E+00
cl-	0.76297028E+00	0.76297750E+00	0.10142291E+06	0.00000000E+00	0.10142230E+06	0.00000000E+00
br-	0.23120312E-08	0.23120530E-08	0.30734215E-03	0.00000000E+00	0.30734031E-03	0.00000000E+00

	Input+Initial	Output+Current	Difference	Rel. Dif.(%)	Del Solid/liq %
ca+2	0.65831897E+10	0.65831891E+10	-0.61020896E+03	-0.92691992E-05	-0.80323464E+01
na+	0.11094083E+07	0.11094017E+07	-0.66053204E+01	-0.59539131E-03	0.25614226E-01
al+3	0.61557645E+01	0.61557525E+01	-0.12000537E-04	-0.19494796E-03	-0.10740226E-01
cs+	0.11078728E-04	0.11078663E-04	-0.65575269E-10	-0.59190250E-03	-0.20934647E+00
sr+2	0.33095612E-04	0.33095416E-04	-0.19627531E-09	-0.59305538E-03	-0.57702580E+00
hco3-	0.64817126E+10	0.64817000E+10	-0.12604520E+05	-0.19446280E-03	-0.27831037E+03
no3-	0.30734446E+00	0.30734263E+00	-0.18260267E-05	-0.59413035E-03	-0.10000000E+03
cl-	0.10142367E+06	0.10142307E+06	-0.60490079E+00	-0.59640988E-03	-0.10000000E+03
br-	0.30734446E-03	0.30734262E-03	-0.18333313E-08	-0.59650702E-03	-0.10000000E+03

D.3. Aqueous concentrations vs. grid blocks at specified times

Unit:
- Aqueous species: Concen. in mol/l

VARIABLES =X, Y, Z, P(bar), Sg, Sl, T(C), pH, h+ ,ca+2 ,na+ ,al+3 ,cs+ ,sr+2 ,hco3- ,no3- ,cl- ,br- ,srco3(aq) ,srno3+ ,sroh+ ,
ZONE T= "0.000000E+00 yr" F=POINT

7.620 20.000 -0.324 0.1010E+01 0.6807 0.3193 25.000 7.2701 0.5772E-07 0.1587E-02 0.3278E-03 0.2020E-13 0.4986E-15 0.4979E-15 0.3222E-02 0.9913E-09 0.3290E-03 0.9972E-12 0.6947E-18 0.2309E-23 0.3792E-21

7.620 20.000 -1.048 0.1011E+01 0.6807 0.3193 25.000 7.2701 0.5772E-07 0.1587E-02 0.3278E-03 0.2020E-13 0.4986E-15 0.4979E-15 0.3222E-02 0.9913E-09 0.3290E-03 0.9972E-12 0.6947E-18 0.2309E-23 0.3792E-21

7.620 20.000 -1.848 0.1011E+01 0.6807 0.3193 25.000 7.2701 0.5772E-07 0.1587E-02 0.3278E-03 0.2020E-13 0.4986E-15 0.4979E-15 0.3222E-02 0.9913E-09 0.3290E-03 0.9972E-12 0.6947E-18 0.2309E-23 0.3792E-21

7.620 20.000 -2.648 0.1011E+01 0.6807 0.3193 25.000 7.2701 0.5772E-07 0.1587E-02 0.3278E-03 0.2020E-13 0.4986E-15 0.4979E-15 0.3222E-02 0.9913E-09 0.3290E-03 0.9972E-12 0.6947E-18 0.2309E-23 0.3792E-21

7.620 20.000 -3.448 0.1011E+01 0.6807 0.3193 25.000 7.2701 0.5772E-07 0.1587E-02 0.3278E-03 0.2020E-13 0.4986E-15 0.4979E-15 0.3222E-02 0.9913E-09 0.3290E-03 0.9972E-12 0.6947E-18 0.2309E-23 0.3792E-21

7.620 20.000 -4.248 0.1011E+01 0.6807 0.3193 25.000 7.2701 0.5772E-07 0.1587E-02 0.3278E-03 0.2020E-13 0.4986E-15 0.4979E-15 0.3222E-02 0.9913E-09 0.3290E-03 0.9972E-12 0.6947E-18 0.2309E-23 0.3792E-21

7.620 20.000 -5.048 0.1011E+01 0.6807 0.3193 25.000 7.2701 0.5772E-07 0.1587E-02 0.3278E-03 0.2020E-13 0.4986E-15 0.4979E-15 0.3222E-02 0.9913E-09 0.3290E-03 0.9972E-12 0.6947E-18 0.2309E-23 0.3792E-21

7.620 20.000 -5.772 0.1011E+01 0.6807 0.3193 25.000 7.2701 0.5772E-07 0.1587E-02 0.3278E-03 0.2020E-13 0.4986E-15 0.4979E-15 0.3222E-02 0.9913E-09 0.3290E-03 0.9972E-12 0.6947E-18 0.2309E-23 0.3792E-21

7.620 20.000 -6.248 0.1011E+01 0.6807 0.3193 25.000 7.2701 0.5772E-07 0.1587E-02 0.3278E-03 0.2020E-13 0.4986E-15 0.4979E-15 0.3222E-02 0.9913E-09 0.3290E-03 0.9972E-12 0.6947E-18 0.2309E-23 0.3792E-21

7.620 20.000 -6.553 0.1011E+01 0.6807 0.3193 25.000 7.2701 0.5772E-07 0.1587E-02 0.3278E-03 0.2020E-13 0.4986E-15 0.4979E-15 0.3222E-02 0.9913E-09 0.3290E-03 0.9972E-12 0.6947E-18 0.2309E-23 0.3792E-21

7.620 20.000 -6.915 0.1011E+01 0.6807 0.3193 25.000 7.2701 0.5772E-07 0.1587E-02 0.3278E-03 0.2020E-13 0.4986E-15 0.4979E-15 0.3222E-02 0.9913E-09 0.3290E-03 0.9972E-12 0.6947E-18 0.2309E-23 0.3792E-21

7.620 20.000 -7.525 0.1011E+01 0.6807 0.3193 25.000 7.2701 0.5772E-07 0.1587E-02 0.3278E-03 0.2020E-13 0.4986E-15 0.4979E-15 0.3222E-02 0.9913E-09 0.3290E-03 0.9972E-12 0.6947E-18 0.2309E-23 0.3792E-21

7.620 20.000 -8.325 0.1011E+01 0.6807 0.3193 25.000 7.2701 0.5772E-07 0.1587E-02 0.3278E-03 0.2020E-13 0.4986E-15 0.4979E-15 0.3222E-02 0.9913E-09 0.3290E-03 0.9972E-12 0.6947E-18 0.2309E-23 0.3792E-21

7.620 20.000 -8.934 0.1011E+01 0.6807 0.3193 25.000 7.2701 0.5772E-07 0.1587E-02 0.3278E-03 0.2020E-13 0.4986E-15 0.4979E-15 0.3222E-02 0.9913E-09 0.3290E-03 0.9972E-12 0.6947E-18 0.2309E-23 0.3792E-21

7.620 20.000 -9.296 0.1012E+01 0.6807 0.3193 25.000 7.2701 0.5772E-07 0.1587E-02 0.3278E-03 0.2020E-13 0.4986E-15 0.4979E-15 0.3222E-02 0.9913E-09 0.3290E-03 0.9972E-12 0.6947E-18 0.2309E-23 0.3792E-21

D.4. Changes of mineral abundance (or/and exchanged species concentrations) vs. grid blocks at specified times

Unit:

- Mineral: Abundance in volume fraction
- Exchanged species: Concentrations in mol/l

```
VARIABLES =X,  Y,  Z,  T(C), Porosity,  Perm(m^2),  calcite  ,gibbsite  ,na+  ,ca+2  ,al+3  ,cs+
  ,sr+2  ,h+  ,
ZONE T= "0.000000E+00 yr"  F=POINT
   7.620   20.000   -0.324  25.000   0.32000  0.91700E-11  0.3400E-01  0.0000E+00  0.4313E-02  0.4375E+00
0.3799E-10  0.4674E-13  0.1409E-12  0.4500E-12
   7.620   20.000   -1.048  25.000   0.32000  0.91700E-11  0.3400E-01  0.0000E+00  0.4313E-02  0.4375E+00
0.3799E-10  0.4674E-13  0.1409E-12  0.4500E-12
   7.620   20.000   -1.848  25.000   0.32000  0.91700E-11  0.3400E-01  0.0000E+00  0.4313E-02  0.4375E+00
0.3799E-10  0.4674E-13  0.1409E-12  0.4500E-12
   7.620   20.000   -2.648  25.000   0.32000  0.91700E-11  0.3400E-01  0.0000E+00  0.4313E-02  0.4375E+00
0.3799E-10  0.4674E-13  0.1409E-12  0.4500E-12
   7.620   20.000   -3.448  25.000   0.32000  0.91700E-11  0.3400E-01  0.0000E+00  0.4313E-02  0.4375E+00
0.3799E-10  0.4674E-13  0.1409E-12  0.4500E-12
   7.620   20.000   -4.248  25.000   0.32000  0.91700E-11  0.3400E-01  0.0000E+00  0.4313E-02  0.4375E+00
0.3799E-10  0.4674E-13  0.1409E-12  0.4500E-12
   7.620   20.000   -5.048  25.000   0.32000  0.91700E-11  0.3400E-01  0.0000E+00  0.4313E-02  0.4375E+00
0.3799E-10  0.4674E-13  0.1409E-12  0.4500E-12
   7.620   20.000   -5.772  25.000   0.32000  0.91700E-11  0.3400E-01  0.0000E+00  0.4313E-02  0.4375E+00
0.3799E-10  0.4674E-13  0.1409E-12  0.4500E-12
   7.620   20.000   -6.248  25.000   0.32000  0.91700E-11  0.3400E-01  0.0000E+00  0.4313E-02  0.4375E+00
0.3799E-10  0.4674E-13  0.1409E-12  0.4500E-12
   7.620   20.000   -6.553  25.000   0.32000  0.91700E-11  0.3400E-01  0.0000E+00  0.4313E-02  0.4375E+00
0.3799E-10  0.4674E-13  0.1409E-12  0.4500E-12
   7.620   20.000   -6.915  25.000   0.32000  0.91700E-11  0.3400E-01  0.0000E+00  0.4313E-02  0.4375E+00
0.3799E-10  0.4674E-13  0.1409E-12  0.4500E-12
   7.620   20.000   -7.525  25.000   0.32000  0.91700E-11  0.3400E-01  0.0000E+00  0.4313E-02  0.4375E+00
0.3799E-10  0.4674E-13  0.1409E-12  0.4500E-12
   7.620   20.000   -8.325  25.000   0.32000  0.91700E-11  0.3400E-01  0.0000E+00  0.4313E-02  0.4375E+00
0.3799E-10  0.4674E-13  0.1409E-12  0.4500E-12
   7.620   20.000   -8.934  25.000   0.32000  0.91700E-11  0.3400E-01  0.0000E+00  0.4313E-02  0.4375E+00
0.3799E-10  0.4674E-13  0.1409E-12  0.4500E-12
```

D.5. Gas vs. grid blocks at specified times

Unit:
- Gas: volume fraction

```
VARIABLES =X,       Y,      Z,   T(C),     P(bar),  co2(g)     ,
ZONE T= "0.000000E+00 yr"  F=POINT
     7.620     20.000    -0.324  25.000  0.1010E+01  0.9896E-02
     7.620     20.000    -1.048  25.000  0.1011E+01  0.9895E-02
     7.620     20.000    -1.848  25.000  0.1011E+01  0.9895E-02
     7.620     20.000    -2.648  25.000  0.1011E+01  0.9894E-02
     7.620     20.000    -3.448  25.000  0.1011E+01  0.9893E-02
     7.620     20.000    -4.248  25.000  0.1011E+01  0.9892E-02
     7.620     20.000    -5.048  25.000  0.1011E+01  0.9891E-02
     7.620     20.000    -5.772  25.000  0.1011E+01  0.9890E-02
     7.620     20.000    -6.248  25.000  0.1011E+01  0.9890E-02
     7.620     20.000    -6.553  25.000  0.1011E+01  0.9889E-02
     7.620     20.000    -6.915  25.000  0.1011E+01  0.9889E-02
     7.620     20.000    -7.525  25.000  0.1011E+01  0.9888E-02
     7.620     20.000    -8.325  25.000  0.1011E+01  0.9887E-02
     7.620     20.000    -8.934  25.000  0.1011E+01  0.9887E-02
     7.620     20.000    -9.296  25.000  0.1012E+01  0.9886E-02
     7.620     20.000    -9.601  25.000  0.1012E+01  0.9886E-02
     7.620     20.000    -9.906  25.000  0.1012E+01  0.9886E-02
     7.620     20.000   -10.270  25.000  0.1012E+01  0.9885E-02
     7.620     20.000   -10.880  25.000  0.1012E+01  0.9884E-02
     7.620     20.000   -11.680  25.000  0.1012E+01  0.9884E-02
     7.620     20.000   -12.290  25.000  0.1012E+01  0.9883E-02
     7.620     20.000   -12.650  25.000  0.1012E+01  0.9882E-02
     7.620     20.000   -12.950  25.000  0.1012E+01  0.9882E-02
     7.620     20.000   -13.260  25.000  0.1012E+01  0.9882E-02
     7.620     20.000   -13.560  25.000  0.1012E+01  0.9881E-02
     7.620     20.000   -13.870  25.000  0.1012E+01  0.9881E-02
     7.620     20.000   -14.170  25.000  0.1012E+01  0.9881E-02
```

D.6. Time evolution at specified elements

Unit:
- Aqueous species: Concen. in mol/l
- Mineral: Abundance in volume fraction
- Gas: volume fraction
- Exchanged species: Concentrations in mol/l

ELEM Time(yr) P(bar) Sg Sl T(C) pH Porosity Perm(m^2) h+ ca+2 na+ al+3 cs+ sr+2 hco3- no3- cl- br- srco3(aq) srno3+ sroh+ calcite gibbsite co2(g) na+ ca+2 al+3 cs+ sr+2 h+

JN114 0.000000E+00 0.1014E+01 0.7522 0.2478 25.000 7.270 0.05000 0.3000E-13 0.5772E-07 0.1587E-02 0.3278E-03 0.2020E-13 0.4986E-15 0.4979E-15 0.3222E-02 0.9913E-09 0.3290E-03 0.9972E-12 0.6947E-18 0.2309E-23 0.3792E-21 0.4750E-01 0.0000E+00 0.9858E-02 0.9939E-04 0.1008E-01 0.8755E-12 0.1077E-14 0.3248E-14 0.1037E-13

ND130 0.000000E+00 0.1024E+01 0.2563 0.7437 25.000 7.270 0.47000 0.2180E-12 0.5772E-07 0.1587E-02 0.3278E-03 0.2020E-13 0.4986E-15 0.4979E-15 0.3222E-02 0.9913E-09 0.3290E-03 0.9972E-12 0.6947E-18 0.2309E-23 0.3792E-21 0.2650E-01 0.0000E+00 0.9769E-02 0.4127E-02 0.4186E+00 0.3635E-10 0.4473E-13 0.1349E-12 0.4307E-12

JI131 0.000000E+00 0.1014E+01 0.7522 0.2478 25.000 7.270 0.05000 0.3000E-13 0.5772E-07 0.1587E-02 0.3278E-03 0.2020E-13 0.4986E-15 0.4979E-15 0.3222E-02 0.9913E-09 0.3290E-03 0.9972E-12 0.6947E-18 0.2309E-23 0.3792E-21 0.4750E-01 0.0000E+00 0.9861E-02 0.9939E-04 0.1008E-01 0.8755E-12 0.1077E-14 0.3248E-14 0.1037E-13

KD132 0.000000E+00 0.1016E+01 0.7589 0.2411 25.000 7.270 0.05000 0.3000E-13 0.5772E-07 0.1587E-02 0.3278E-03 0.2020E-13 0.4986E-15 0.4979E-15 0.3222E-02 0.9913E-09 0.3290E-03 0.9972E-12 0.6947E-18 0.2309E-23 0.3792E-21 0.4750E-01 0.0000E+00 0.9847E-02 0.1021E-03 0.1036E-01 0.8997E-12 0.1107E-14 0.3338E-14 0.1066E-13

KH132 0.000000E+00 0.1016E+01 0.1473 0.8527 25.000 7.270 0.47000 0.2180E-12 0.5772E-07 0.1587E-02 0.3278E-03 0.2020E-13 0.4986E-15 0.4979E-15 0.3222E-02 0.9913E-09 0.3290E-03 0.9972E-12 0.6947E-18 0.2309E-23 0.3792E-21 0.2650E-01 0.0000E+00 0.9845E-02 0.3600E-02 0.3651E+00 0.3171E-10 0.3902E-13 0.1176E-12 0.3756E-12

JF133 0.000000E+00 0.1014E+01 0.7530 0.2470 25.000 7.270 0.05000 0.3000E-13 0.5772E-07 0.1587E-02 0.3278E-03 0.2020E-13 0.4986E-15 0.4979E-15 0.3222E-02 0.9913E-09 0.3290E-03 0.9972E-12 0.6947E-18 0.2309E-23 0.3792E-21 0.4750E-01 0.0000E+00 0.9866E-02 0.9971E-04 0.1011E-01 0.8783E-12 0.1081E-14 0.3259E-14 0.1041E-13

KE136 0.000000E+00 0.1016E+01 0.8351 0.1649 25.000 7.270 0.05000 0.3000E-13 0.5772E-07 0.1587E-02 0.3278E-03 0.2020E-13 0.4986E-15 0.4979E-15 0.3222E-02 0.9913E-09 0.3290E-03 0.9972E-12 0.6947E-18 0.2309E-23 0.3792E-21 0.4750E-01 0.0000E+00 0.9847E-02 0.1493E-03 0.1515E-01 0.1315E-11 0.1619E-14 0.4880E-14 0.1558E-13

IU137 0.000000E+00 0.1012E+01 0.6803 0.3197 25.000 7.270 0.32000 0.9170E-11 0.5772E-07 0.1587E-02 0.3278E-03 0.2020E-13 0.4986E-15 0.4979E-15 0.3222E-02 0.9913E-09 0.3290E-03 0.9972E-12 0.6947E-18 0.2309E-23 0.3792E-21 0.3400E-01 0.0000E+00 0.9880E-02 0.4308E-02 0.4369E+00 0.3794E-10 0.4669E-13 0.1408E-12 0.4495E-12

J4137 0.000000E+00 0.1012E+01 0.7530 0.2470 25.000 7.270 0.05000 0.3000E-13 0.5772E-07 0.1587E-02 0.3278E-03 0.2020E-13 0.4986E-15 0.4979E-15 0.3222E-02 0.9913E-09 0.3290E-03 0.9972E-12 0.6947E-18 0.2309E-23 0.3792E-21 0.4750E-01 0.0000E+00 0.9877E-02 0.9971E-04 0.1011E-01 0.8783E-12 0.1081E-14 0.3259E-14 0.1041E-13

KF137 0.000000E+00 0.1016E+01 0.2225 0.7775 25.000 7.270 0.47000 0.2180E-12 0.5772E-07 0.1587E-02 0.3278E-03 0.2020E-13 0.4986E-15 0.4979E-15 0.3222E-02 0.9913E-09 0.3290E-03 0.9972E-12 0.6947E-18 0.2309E-23 0.3792E-21 0.2650E-01 0.0000E+00 0.9846E-02 0.3948E-02 0.4004E+00 0.3477E-10 0.4279E-13 0.1290E-12 0.4120E-12

E. EFFECT OF SIDE-BOUNDARY CONDITION TEST

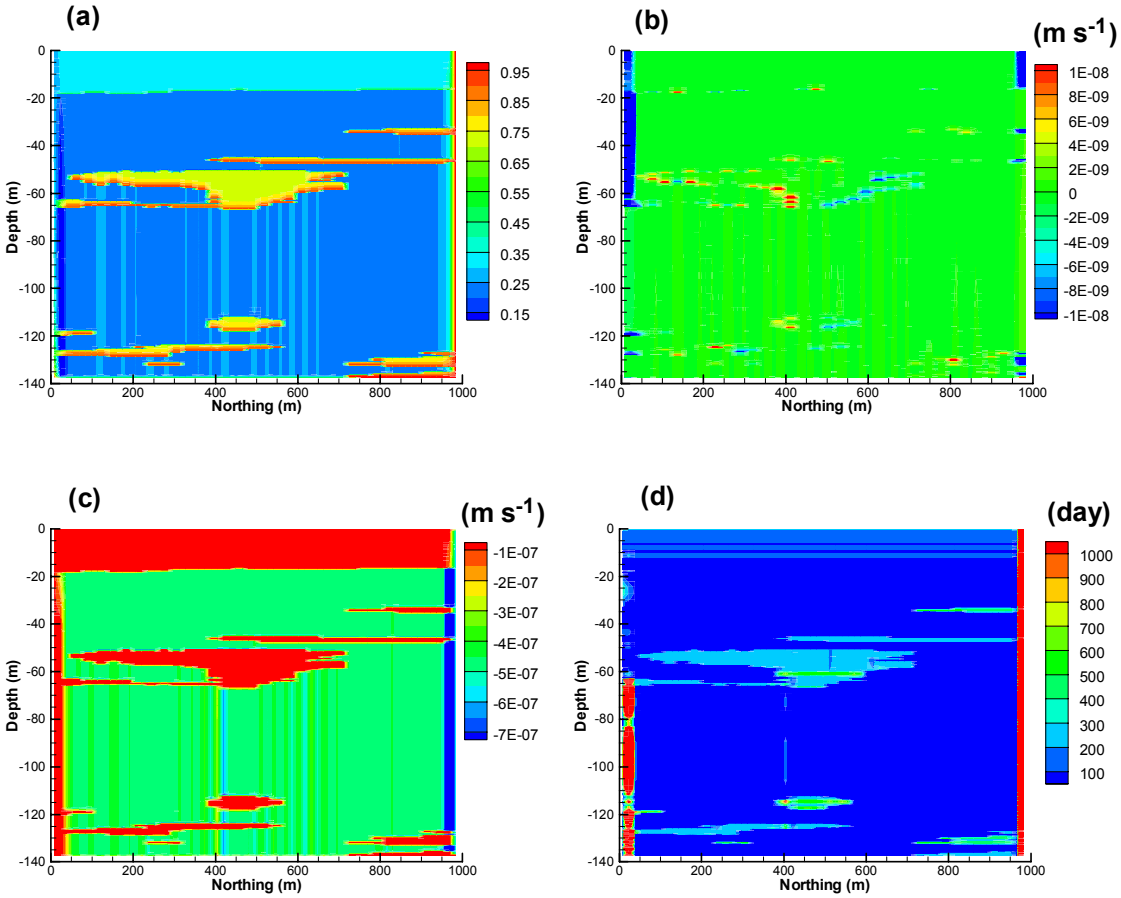

Figure E.1. Steady-state water flow field by assuming a 100k times greater vertical permeability for grid blocks along the left side boundary, and a constant water saturation of 0.96 along the right side boundary, with other parameterization kept the same as in the base run. (a) water saturation, (b) horizontal pore-water velocity, (c) vertical pore-water velocity, (d) water residence time.

F. Distribution coefficient and retardation factor for strontium with space and time

It was shown that both distribution coefficient and retardation factor for Sr^{2+} changed with material, as well as over time, with the changing of concentrations of Sr^{2+} and competing ions in solution and on exchange sites (Fig. F.1, F.2).

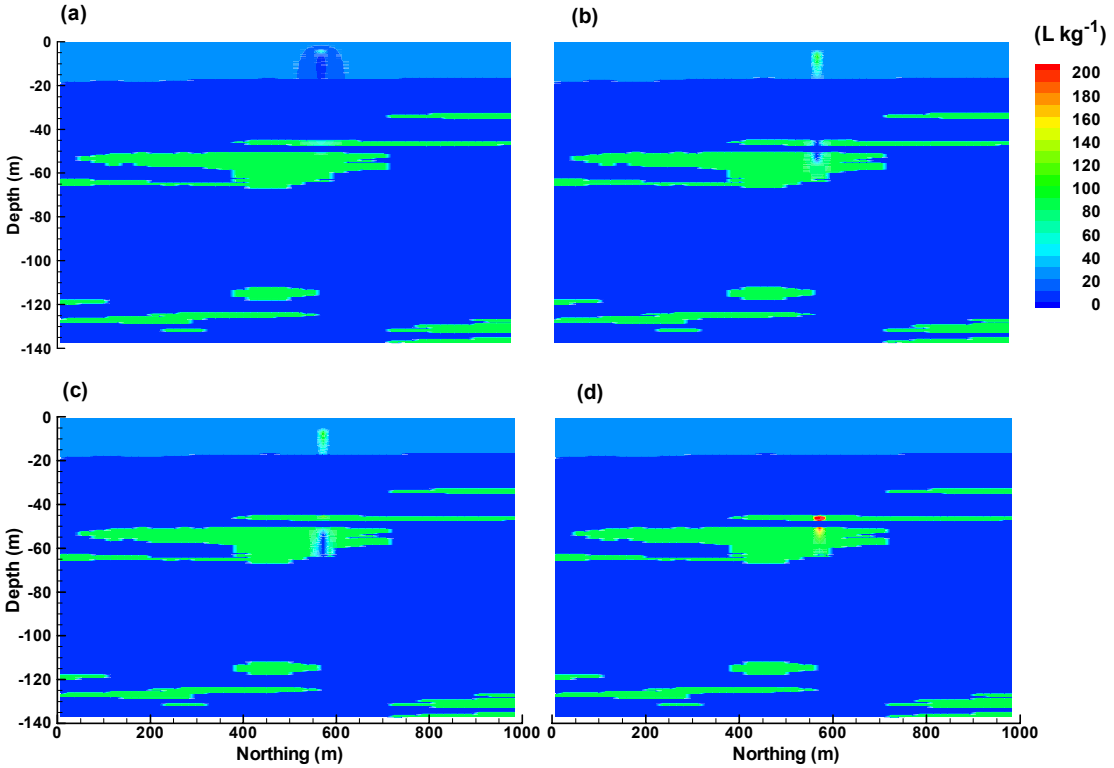

Figure F.1. Distribution coefficient for strontium in base run at (a) 5, (b) 15, (c) 30, and (d) 200 yr.

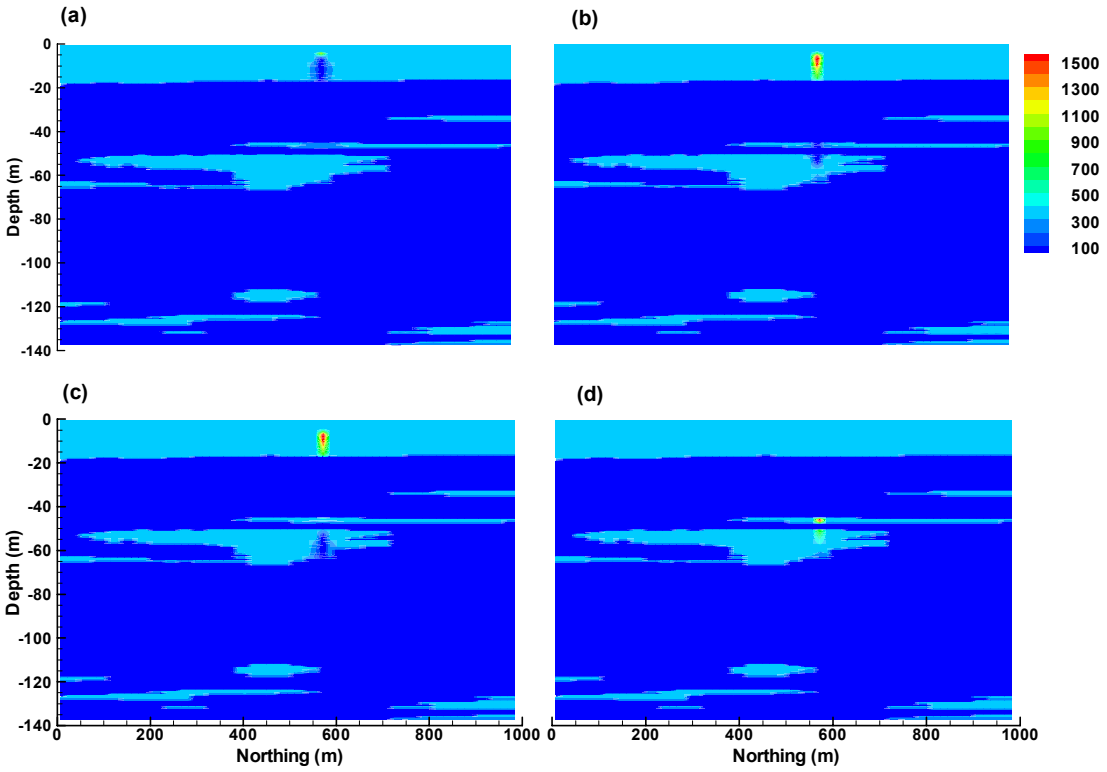

F.2. Retardation factor for strontium in base run at (a) 5, (b) 15, (c) 30, and (d) 200 yr.